Evaluating the impact of climate change and millennial variability on the last Neanderthal populations in Europe (Marine Isotope Stage 3)

Benjamin Albouy, Simon Paquin, Julien Riel-Salvatore, Masa Kageyama, Mathieu Vrac, Ariane Burke

Quaternary Science Reviews 338 (2024) 108812

Contents lists available at ScienceDirect

Quaternary Science Reviews

journal homepage: www.elsevier.com/locate/quascirev

Evaluating the impact of climate change and millennial variability on the last Neanderthal populations in Europe (Marine Isotope Stage 3)

Benjamin Albouy [a,*], Simon Paquin [a], Julien Riel-Salvatore [a], Masa Kageyama [b], Mathieu Vrac [b], Ariane Burke [a]

[a] Département D'anthropologie, Université de Montréal Pavillon Lionel-Groulx, 3150 Jean-Brillant, Montréal, QC, H3T 1N8, Canada
[b] Laboratoire des Sciences Du Climat et de L'Environnement (LSCE-IPSL), Centre D'Études de Saclay, Orme des Merisiers, Bat. 714, 91191 Gif-sur-Yvette, France

ARTICLE INFO

Keywords:
Homo neanderthalensis
Late pleistocene
Europe
Paleoclimate modeling
Species distribution modeling
Random forest
Habitat suitability

ABSTRACT

Present in Eurasia since 350 ka BP, Neanderthals show several adaptive strategies to long-term climate change. Their disappearance from the archaeological and fossil record around 40 ka BP, during a period of climate instability, raises the question of the role of climate variability on their resilience, and potentially on their extinction. In this research, we built habitat suitability models for Neanderthal populations in Europe under stadial and interstadial conditions of Marine Isotope Stage 3 (MIS 3). To do so, we apply species distribution modelling using Random Forest to test a wide range of predictors linked to topography, climate change and climate variability, at high spatial (15 km × 15 km) and temporal (annual, seasonal) resolution. This approach allows us to compare the variables influencing habitat suitability during stadial and interstadial phases and discuss the implications of millennial-scale climate change on the spatial distribution of Neanderthal populations in Europe during MIS 3. We identify key environmental stressors and investigate the role of ecological risk in shaping the spatial distribution of Neanderthals and finally, discuss their resilience and the factors leading to their eventual extinction.

1. Introduction

The archaeological and paleoanthropological records testify to the fact that Neanderthals (*Homo neanderthalensis*) were present across Eurasia, from Western Europe to Siberia (Serangeli and Bolus, 2008), from 350 thousand years Before Present (ka BP) (Hublin, 2009) to 40 ka BP (Higham et al., 2014). The archaeological record also shows that Neanderthals were a highly adaptive species (Roebroeks and Soressi, 2016) with advanced technological (e.g., Delagnes et al., 2007) and subsistence skills (e.g., Burke, 2000; Patou-Mathis, 2000; Fiorenza et al., 2015) in addition to symbolic behavior (e.g., d'Errico et al., 1998; Soressi and d'Errico, 2007; Rendu et al., 2014).

Neanderthal populations disappear from the fossil record during MIS 3 (Higham et al., 2014; Devièse et al., 2021; Heydari-Guran et al., 2021). This period was marked by a global cooling trend, punctuated by a series of abrupt climatic changes (Sánchez Goñi and Harrison, 2010). In Europe, it also coincides with the arrival of anatomical modern humans, *Homo sapiens*, from the Near East (Hublin, 2015) possibly as early as 54 ka BP (Slimak et al., 2022). These climatic and demographic factors could have had important consequences for Neanderthal populations (Hublin, 2009; Albouy et al., 2023), possibly leading to their extinction (d'Errico and Sánchez Goñi, 2003; van Andel and Davies, 2003; Banks et al., 2008a; Melchionna, 2018; Melchionna et al., 2018).

In this research, we assess the resilience of Neanderthal populations and the influence of millennial-scale climate variability on their spatial distribution. To do so, we rely on archaeological data, climate simulations and the construction of habitat suitability models.

1.1. MIS 3 and millennial climate variability

MIS 3 extends from 59,4 ka to 27,8 ka BP (Svensson et al., 2006, 2008; Sánchez Goñi and Harrison, 2010, p. 2825). It is a period marked by a strong, millennial-scale climatic instability (Wolff et al., 2010). This instability was the consequence of two types of climate event that affected the Northern Hemisphere, particularly during the Last Ice Age: Dansgaard-Oeschger cycles (D-O) (Dansgaard et al., 1984) and Heinrich

* Corresponding author.
E-mail addresses: benjamin.albouy@umontreal.ca (B. Albouy), simon.paquin@umontreal.ca (S. Paquin), julien.riel-salvatore@umontreal.ca (J. Riel-Salvatore), masa.kageyama@lsce.ipsl.fr (M. Kageyama), mathieu.vrac@lsce.ipsl.fr (M. Vrac), a.burke@umontreal.ca (A. Burke).

https://doi.org/10.1016/j.quascirev.2024.108812
Received 25 April 2024; Received in revised form 29 June 2024; Accepted 1 July 2024
Available online 17 July 2024

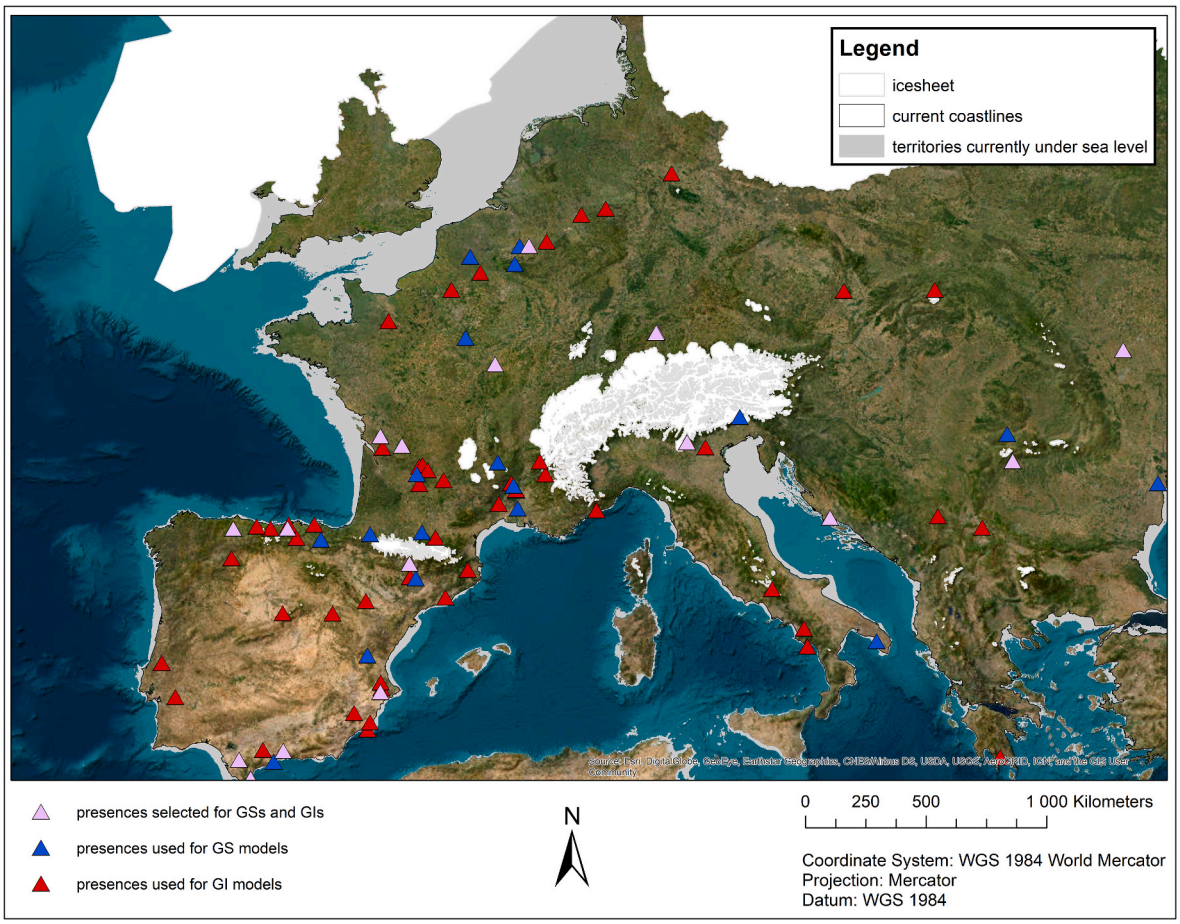

Fig. 1. Distribution of presences used for modeling process. ESRI's World Imagery Map was used as the base map for this figure. The extent of the glaciers is based on Ehlers et al.'s (2011) reconstruction. This reconstruction represents the Late Glacial Maximum, but it has been utilized as a proxy for the maximum extent of the ice sheet during stadial periods of the MIS 3 (Paquin et al., 2024). The extent of the MIS 3 coastline is based on a reconstruction suggested in prior research (Albouy et al., 2023).

events (Heinrich, 1988).

D-O cycles identified in the Greenland ice cores (NGRIP, GISP2, GRIP) are characterized by abrupt warming followed by a cooling period (Dansgaard et al., 1993). The warming phases last around 60 years while cooling phases can last more than 2 ka, including an initial slow cooling, a more abrupt cooling and a slower final cooling (Sánchez Goñi and Harrison, 2010). Nineteen stadial (GS)/interstadial (GI) cycles have been identified during MIS 3 (Rasmussen et al., 2014), sometimes associated with Heinrich events (Heinrich, 1988), short-term climate events associated with lower sea-surface temperatures and a cooler continental climate, called Heinrich stadials (Sánchez Goñi and Harrison, 2010). Readers may refer to Albouy et al. (2023) - Supplement material 4 for an overview of the chronological relationship between Heinrich stadials and GSs/GIs during MIS 3.

1.2. Neanderthal and climate fluctuations

Climate fluctuations, both long term (climate change) or short term (climate variability) have impacted the dispersal of hominins and the (internal) dynamics of hominin groups and may have affected the long-term viability of Neanderthal populations in Europe.

Neanderthals show several adaptive strategies to long-term climatic change. These include demographic shifts, e.g., retreats to more temperate zones during glacial periods (Serangeli and Bolus, 2008; Hublin and Roebroeks, 2009), such as the Mediterranean coasts of Europe (see Benito et al., 2017 for MIS 5e). They also developed specific local cultural adaptations that enabled them to persist under less favorable conditions (see Banks et al., 2021 for MIS 5e and MIS 4).

They also show several adaptative responses to short-term climate fluctuations, particularly during MIS 3, such as seasonal mobility (e.g., Delagnes and Rendu, 2011; Riel-Salvatore et al., 2013), the seasonal management of resources (e.g., Rendu, 2007; Fernández-Laso et al., 2010; Conard et al., 2012; Daujeard et al., 2012; Rendu et al., 2012), and resource substitutions (e.g., Martínez et al., 2005; Vallverdú et al., 2005). These observations lead us to consider that climate variability could have had a decisive influence on their spatial behavior. Climate variability may have led to changes in habitat use which would have directly impacted demographics, information flow, and cultural transmission as observed in hunter-gatherers ethnographic record (Ember and Ember, 1992; Winterhalder et al., 1999; Collard et al., 2011; Kelly, 2013). The combination of all these factors could have tested their resilience and ultimately led to their decline or even extinction.

This research is designed to study Neanderthal spatial behavior at both scales, taking into account climate change and climate variability. The models use the appropriate forcings for stadial and interstadial conditions during MIS 3 and the resulting simulations capture the essential difference between these two climate states.

1.3. New tools, new scales

Thanks to recent advances in paleoclimatic modeling (see Burke and Riede, 2023 for a general review) it is now possible to simulate long-term trends (climate change), and short-term climate fluctuations (climate variability) and examine their impact on hominin populations.

These new data and tools allow us to consider past environments at smaller, and therefore more human, scales, both temporally (yearly or seasonally) and spatially (i.e., 15 km by 15 km; a typical human foraging radius) (Vita-Finzi et al., 1970).

Species distribution models (SDMs) are increasingly used in archaeology to study the impact of climatic fluctuations on Pleistocene human populations, particularly in Europe (van Andel and Davies, 2003; Banks et al., 2006, 2008a, 2008b, 2011, 2013, 2021; Grove, 2011; Bradtmöller et al., 2012; Burjachs et al., 2012; Schmidt et al., 2012; Burke et al., 2014, 2017; Tallavaara et al., 2015; Banks, 2017; Ludwig et al., 2018; Melchionna, 2018; Melchionna et al., 2018; Sepulchre et al., 2007; Franklin et al., 2015; Timmermann and Friedrich, 2016; Benito et al., 2017; Timmermann, 2020; Ordonez and Riede, 2022; Klein et al., 2023; Yaworsky et al., 2024). Much of this research has focussed on the impact of climate change on Neanderthal populations (Benito et al., 2017; Banks et al., 2021; Yaworsky et al., 2024) but several papers have studied the impact of small-scale climate fluctuations, specifically during MIS 3 (Sepulchre et al., 2007; Banks et al., 2008a; Melchionna, 2018; Melchionna et al., 2018; Timmermann, 2020).

In this research, we employ the SDM with Random Forest (RF) methodology, following the protocol established by the Hominin Dispersal Research Group (Burke et al., 2017; Paquin et al., 2024), to construct habitat suitability for Neanderthals during GSs and GIs.

The "niche" concept is a subject of debate in ecology. Here, we use the term "habitat", adopting the definition given by Kearney (2006, p. 187): "Habitat is a description of a physical place, at a particular scale of space and time, where an organism either actually or potentially lives". According to this definition, habitat takes into account abiotic factors and mobility in the absence of information on biotic interactions, as opposed to the ecological niche that includes these factors.

In our research, we address two pivotal research questions: 1) what is the impact of large-scale climate change (i.e., GS and GI) on the distribution of suitable habitat? and 2) what is the impact of climate variability within each of these two climate phases?

The results presented here allow us to discuss the various hypotheses proposed in the literature regarding the resilience of Neanderthal populations and the climatic factors that may have ultimately caused their extinction, including: the contraction (Serangeli and Bolus, 2008; Hublin, 2009; Albouy et al., 2023) and fragmentation (Melchionna, 2018; Melchionna et al., 2018; Albouy et al., 2023) of suitable habitat.

2. Material and methods

2.1. Archaeological data

The spatial location of archaeological sites is a proxy for the distribution of human populations. For this research we use an updated database of Neanderthal paleogeography during MIS 3 described in detail in a previous paper (Albouy et al., 2023) and summarized below. The geographical domain includes Europe, from 32.7 decimal degree (DD) South to 60.0 DD North and 12.6 DD West to 35.0 DD East, as illustrated in Fig. 1. The temporal boundaries of the dataset are between GI-17.2 (59,44 b2k), i.e., the beginning of MIS 3 (Rasmussen et al., 2014), and the end of GS-9 (38,221 b2k) (Rasmussen et al., 2014), when Neanderthals are considered to have become extinct (Higham et al., 2014). We retained all archaeological sites containing Mousterian industries and/or Neanderthal remains, eliminating sites with transitional industries that fall within our time frame because there are too many uncertainties regarding their chronology, the homogeneity and taphonomic integrity of the assemblages, and their association with a specific human taxon (see Albouy et al., 2023 for a detailed discussion of these points).

The data compilation consisted in four steps.

(1) the identification and collection of archaeological data from existing databases, including *S2AGES* (Pettitt et al., 2003); *PACEA geo-referenced radiocarbon database* (d'Errico et al., 2011) and the *Palaeolithic Europe Database v20* (Vermeersch, 2019) and the collection of additional data from recent publications [up to December 2021];
(2) integration of these data into a new database, homogenization of the data and the addition of complementary paleoenvironmental information.
(3) verification of the reliability of the reported dates and;
(4) verification of the site coordinates.

Then, we proceeded to select reliably dated archaeological sites from the database following three steps.

(1) the preselection of the dates following a taphonomic analysis, to evaluate the homogeneity and the reliability of each date;
(2) the chronological Bayesian modeling of the retained dates, taking into account the different dating methods used; we modeled the probability that an individual archaeological layer falls within a cold (stadial) or a warm (interstadial) climatic interval as defined by Rasmussen et al. (2014) using a script built by our research team (Albouy et al., 2023; Paquin et al., 2023). In the event that a layer was dated within more than one temporal interval, the interval with the maximum probability mass was retained (for more details on our methodology, see Albouy et al., 2023);
(3) calculation of an uncertainty estimate for each site, taking into account the number of dates used for each chronological model, the associated paleoenvironmental data, and the stratigraphic coherence of the different layers, in case of multilayered sites.

Following this methodology, we obtained two datasets containing dated, archaeological layers that could be associated with a GS or a GI, and their uncertainty scores (see Albouy et al., 2023). The sites with the highest scores (scores 2 and 3) were used as presences in the habitat suitability models. We were thus able to identify a total of 35 unique presences for GSs and 72 unique presences for GIs for use in the modeling process (Fig. 1 and SI 1).

2.2. Candidate predictors

2.2.1. Simulated climate variables

Traditional climate proxies, i.e., paleoenvironmental data such as pollen or charcoal, are subject to biases due to their differential distribution and poor chronological control. Therefore, and in collaboration with the *Laboratoire des Sciences du Climat et de l'Environement* (UMR 8212), we used climate simulations to provide climate predictors. Two global climate simulations for MIS 3 GS and GI were created using a global Atmosphere-Ocean General Circulation Model (IPSL-CM5A-LR) (Dufresne et al., 2013) following the PMIP3 protocol (Braconnot et al., 2012; Kageyama et al., 2013). The simulation's outputs were used to extract a 50-year time series of monthly averages for the following variables: air temperature at 2 m above sea level, sea-level pressure, surface wind, relative humidity, and cloud cover fraction. Non-linear statistical downscaling was applied to these data using a Generalized Additive Model (GAM) to achieve a spatial scale of $\sim$15 $\times$ 15 km (Vrac et al., 2007; Latombe et al., 2018). Readers interested in further details on this methodology and its theoretical and technical aspects are referred to Paquin et al. (2024).

2.2.2. Predictive variables

We derived three types of predictive variable under GS and GI conditions: 1) geographical variables, 2) climate variables, and 3) climate variability indices following the protocol established in Burke et al. (2017) and Paquin et al. (2024).

1) Geographical variables, such as elevation and slope were obtained from the SRTM 90-m digital elevation model (DEM) resampled at a 1

Table 1
List of candidate predictors (N = 40). This table includes the type of predictor (topographical, climatological and climate variability), the data source, and a brief description adapted from Burke et al. (2017). X = selected by autocorrelation. (+)/(−) = manual adjustments (see Paquin et al., 2024; **SI 3** for details).

Predictor	Type	Derivation	Description	Selection	
				GS	GI
elev	Topographic	DEM[a]	elevation (m *asl*)	X	X
slope	Topographic	DEM[a]	slope (reclassified) (degree)	X	X
p_avg_aut	Climatology	Climate simulation	Seasonal precipitation average, autumn (mm)		
p_avg_spr	Climatology	Climate simulation	Seasonal precipitation average, spring (mm)		
p_avg_sum	Climatology	Climate simulation	Seasonal precipitation average, summer (mm)		X
p_avg_win	Climatology	Climate simulation	Seasonal precipitation average, winter (mm)		
p_avg_y	Climatology	Climate simulation	Annual precipitation average (mm)	X	X
p_max_aut	Climatology	Climate simulation	Seasonal precipitation maximum, autumn (mm)	X	X
p_max_spr	Climatology	Climate simulation	Seasonal precipitation maximum, spring (mm)	X	X
p_max_sum	Climatology	Climate simulation	Seasonal precipitation maximum, summer (mm)	X	X
p_max_win	Climatology	Climate simulation	Seasonal precipitation maximum, winter (mm)	X	X
p_min_aut	Climatology	Climate simulation	Seasonal precipitation minimum, autumn (mm)	X	X
p_min_spr	Climatology	Climate simulation	Seasonal precipitation minimum, spring (mm)	X	X
p_min_sum	Climatology	Climate simulation	Seasonal precipitation minimum, summer (mm)	X	X
p_min_win	Climatology	Climate simulation	Seasonal precipitation minimum, winter (mm)	X	X
p_var_aut	Climate variability	Climate simulation	Seasonal precipitation, coeff. var., autumn	X	X
p_var_spr	Climate variability	Climate simulation	Seasonal precipitation, coeff. var., spring	X	X
p_var_sum	Climate variability	Climate simulation	Seasonal precipitation, coeff. var., summer	X	X
p_var_win	Climate variability	Climate simulation	Seasonal precipitation, coeff. var., winter	X	X
p_var_y	Climate variability	Climate simulation	Seasonal precipitation, coeff. var., yearly		X
spi_norm[b]	Climate variability	Climate simulation	N months within normal (predicted) range	X	X
sti_norm[c]	Climate variability	Climate simulation	N months within normal (predicted) range	X	X
t_avg_aut	Climatology	Climate simulation	Seasonal temperature average, autumn (°C/10)	(+)	(+)
t_avg_spr	Climatology	Climate simulation	Seasonal temperature average, spring (°C/10)		
t_avg_sum	Climatology	Climate simulation	Seasonal temperature average, summer (°C/10)		
t_avg_win	Climatology	Climate simulation	Seasonal temperature average, winter (°C/10)		
t_avg_y	Climatology	Climate simulation	Yearly temperature average (°C/10)		
t_max_aut	Climatology	Climate simulation	Seasonal temperature maximum, autumn (°C/10)		
t_max_spr	Climatology	Climate simulation	Seasonal temperature maximum, spring (°C/10)		X
t_max_sum	Climatology	Climate simulation	Seasonal temperature maximum, summer (°C/10)		
t_max_win	Climatology	Climate simulation	Seasonal temperature maximum, winter (°C/10)		(−)
t_min_aut	Climatology	Climate simulation	Seasonal temperature minimum, winter (°C/10)		
t_min_spr	Climatology	Climate simulation	Seasonal temperature minimum, spring (°C/10)		
t_min_sum	Climatology	Climate simulation	Seasonal temperature minimum, summer (°C/10)	X	X
t_min_win	Climatology	Climate simulation	Seasonal temperature minimum, winter (°C/10)		
t_sd_aut	Climate variability	Climate simulation	Standard deviation, seasonal temperature, autumn	(+)	(+)
t_sd_spr	Climate variability	Climate simulation	Standard deviation, seasonal temperature, spring		
t_sd_sum	Climate variability	Climate simulation	Standard deviation, seasonal temperature, summer	X	X
t_sd_win	Climate variability	Climate simulation	Standard deviation, seasonal temperature, winter	X	X
t_sd_y	Climate variability	Climate simulation	Standard deviation, temperature, yearly		

[a] DEM = Digital Elevation Model.
[b] SPI = Standardized Precipitation Index.

[c] STI = Standardized Temperature Index.

× 1 km scale using ArcMap (v. 10.8.1). In the absence of palaeotopographic reconstructions at an appropriate scale, we elected to use modern topographic data.

2) Climate variables: annual, seasonal and monthly averages, minima and maxima were calculated from 50-year runs of simulated climate variables for temperature and precipitation.
3) Climate variability: we also used the simulated climate variables to calculate several indices of climate variability including: the standard deviation (temperature), the coefficient of variability (precipitation), the Standard Precipitation Index (SPI), and the Standardized Temperature Index (STI). The Standardized Precipitation Index (SPI) (McKee et al., 1993; Guttman, 1999; Hayes, 2000) was calculated using the *SPEI* package in R (Vicente-Serrano et al., 2010) while the Standardized Temperature Index (STI) was calculated using the *STI* package in R (Fasel, 2015).

The initial candidate predictors (N = 40) are listed in Table 1.

2.2.3. Preparation of datasets

The climate predictors were interpolated using the *Natural Neighbor* tool and resampled in ArcMap to create a raster with a resolution of 1 km per 1 km. The resulting rasters were clipped using a Holocene coastal mask reflecting the lack of archaeological surveys on currently submerged Pleistocene land masses, and a mask representing the ice sheets during their maximum extension, i.e., MIS 3 GSs, from Ehlers et al. (2011) (Fig. 1).

A 1 km scale point feature class was created in ArcMap and the georeferenced archaeological sites (presences) were loaded into this point feature class. In order to prevent the occurrence of multiple observations, we have retained only one presence when several layers documented the same climate phase. Furthermore, sites within 2 km of each other were considered as a single presence. As a result, 35 presences were retained for GSs and 67 presences for GIs. Archaeological sites are discrete locations, but hunter-gatherers exploit daily catchment areas that have a roughly 10 km radius. We therefore apply a 10-km buffer around the sites in order to capture each catchment only once. Predictor values were extracted to the resulting point feature class for use in the modeling process.

To remove highly correlated variables, we conducted an autocorrelation test using the *findCorrelation* function in the *caret* R package (version 6.0.96) developed by Kuhn et al. (2022). Correlated predictors with a correlation coefficient greater than 0.8 were manually removed (see Paquin et al., 2024; SI 3 for details). After this procedure, 23 predictors were tested for GSs and 25 predictors were tested for GIs. Table 1, column **Selection**, indicates the list of final candidate predictors chosen for the GS and GI models.

2.3. Modeling method

2.3.1. Random forest

To build predictive models of habitat suitability, we employ RF using regression trees. RF is a nonparametric tool developed by Breiman (2001) that can be utilized for variable selection. This method is a popular alternative to linear regression models and allows us to consider a large number of predictors, relatively few observations and non-linear relationships (Grömping, 2009; Genuer et al., 2010). RF involves building multiple classification trees where each tree is a random subset of the observations, and each split within each tree is a random subset of a prescribed number of randomly selected candidate variables (Grömping, 2009). The final model for each run averages the results obtained for each tree within the final forest. Compared to other modeling methods currently in use, RF provides good average prediction performance (Couronné et al., 2018).

The RF analysis was conducted using the *randomForest* package (Cutler and Wiener, 2022) and run on R software version 4.3.3 (R Core Team, 2024) implemented in R-Studio version 2023.12.1 (RStudio Team, 2023) (see **SI 2**). Default values were used for several model parameters, including the number of trees grown (n-tree = 500) and a 10-fold cross-validation. The number of randomly selected pseudo-absences was set equal to the number of presences, following Barbet-Massin et al. (2012). To enhance the sensitivity of our models, we increased the m. try value, which is the number of input variables randomly selected at each split, as suggested by Genuer et al. (2010) setting mtry = p from the first runs (*23var* model for GSs and *25var* model for GIs). We executed RF 100 times per run and computed the average results to generate the final model.

Outputs include two standard metrics: accuracy (a performance metric based on a confusion matrix) and the out-of-the-bag error rate (OOB) which is calculated internally in RF (Liaw and Wiener, 2002). When building a RF model, a portion of the data (30% in our case) is not included in the bootstrap sample used to form an individual tree, this is the out-of-bag (OOB) sample. Model predictions based on the bootstrap sample are compared with the OOB data for each tree to compute the OOB metric. Both accuracy and OOB are commonly used to evaluate model performance in RF (e.g., Liaw and Wiener, 2002; Elith and Leathwick, 2009; Fox et al., 2017). The model also calculates the Variable Importance (VI) index which is used in the variable selection process. Density plots for the selected variables are included.

2.3.2. Model iteration and selection

A nested series of RF runs was performed to identify the model with the best performance and most parsimonious list of predictors (*ff*. Díaz-Uriarte and Alvarez de Andrés, 2006; Genuer et al., 2010). After each run, candidate predictors were ranked based on their average VI scores (AVI). The bottom 20% was removed in the following run, and the process was repeated until only two predictors remained. The best model was selected based on overall performance (OOB and accuracy) and the number of predictors tested (see **SI 3** for the detailed results).

2.4. Analyzing and mapping the results

After selecting the final models, we created habitat suitability maps in ArcMap. These maps show the mean model predictions for each cell in the spatial extent. To create them, we interpolated the model output point features using the *Natural Neighbor* tool in *Spatial Analyst*. We produced two habitat suitability maps, one for GS and one for GI. Finally, we applied the ice sheet and coastal masks.

As recommended by Klein et al. (2023) and Paquin et al. (2024), we conducted a Generalized Linear Model (GLM) using the predictors retained for GSs and GIs final models to test for collinearity. To do this, we utilized the *GLM* function from the *caret* package in R (Kuhn et al., 2022). The number of pseudo-absences was set to be 10 times greater than the number of presences, as recommended by Wisz and Guisan (2009). The model was run 100 times, and the Variation Inflation Factor (VIF) was calculated for the retained variables. VIF values < 5 indicate that collinearity is negligible. Further detailed information on GLM tests can be found in **SI 3**.

Finally, we mapped the predictors that were retained in the final RF models. This allows for a visual comparison of the distribution of predictors between GSs and GIs (see **SI 4**). Bar plots were created using the *ggplot2* package in R (Wickham, 2016) to compare the distribution of habitat suitability in Europe between GSs and GIs. Density plots were created using the same package to compare the distribution of predictors associated with presences and pseudo-absences.

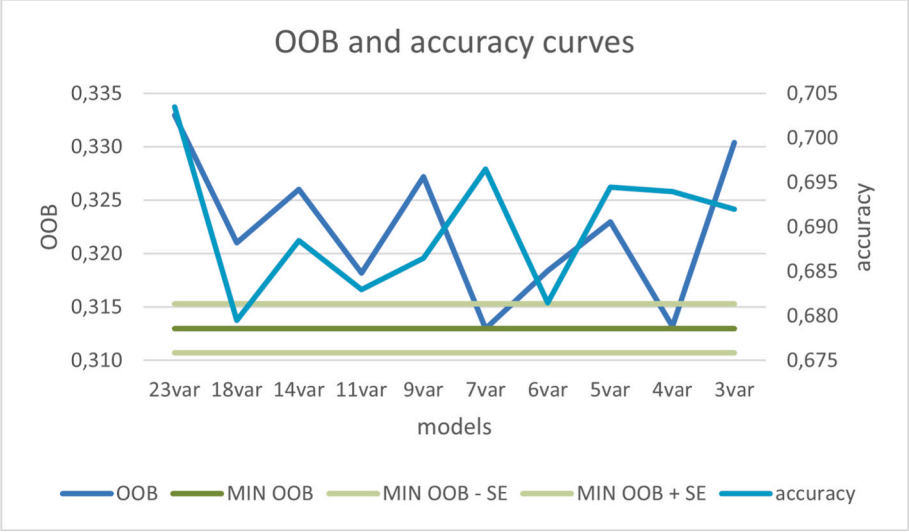

Fig. 2. Model performance indices for GSs models. OOB and accuracy values were extracted and averaged for each model run. The dark green line indicates the lowest OOB value (MIN = 0,3130), while the light green lines indicate one standard error from this value (SE = 0,0023). The results are rounded to the nearest 10e-4.

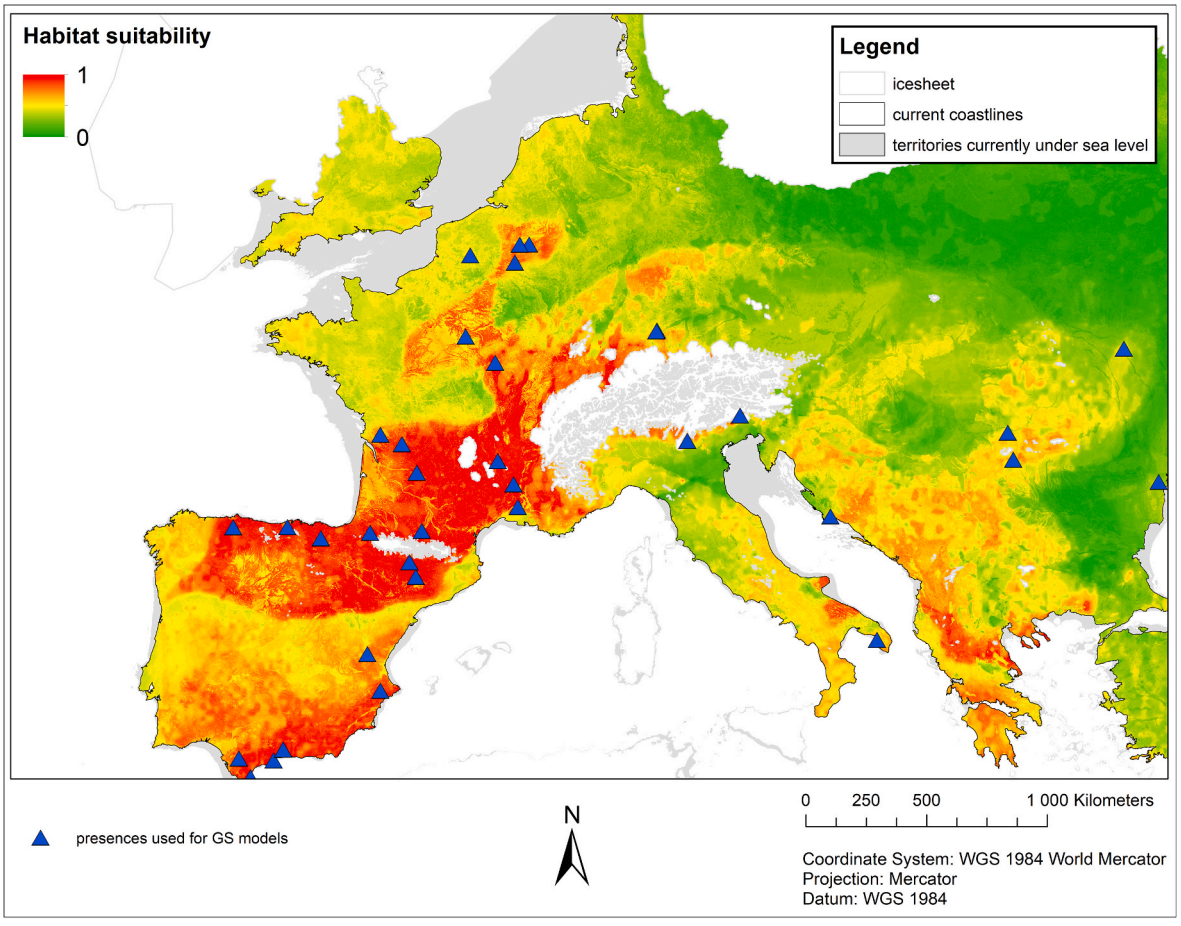

Fig. 3. Habitat suitability model for GSs. The habitat suitability model generated by the *4var* model and retained as the final model for GSs is displayed with the sites utilized as presences.

3. Results

3.1. GSs models

Two models have the best combination of low OOB and high Accuracy values (Fig. 2): *7var* and *4var*. We select the more parsimonious model, *4var,* as the final model for habitat suitability during GSs (Fig. 3). The VIF values indicate that the predictors retained exhibit a negligible degree of collinearity, with a value < 5 for each predictor.

The predictors included in the selected model are, in order of

Table 2
Averaged Variable Importance (AVI) for GS models. Variable importance values were extracted and averaged for each model run and for each predictor. The results are rounded to the nearest 10e-1.

23var		18var		14var		11var		9var		7var		6var		5var		4var		3var	
sti_norm	66,2	p_min_aut	49,1	p_min_aut	57,0	sti_norm	52,7	sti_norm	56,7	sti_norm	59,3	sti_norm	64,2	sti_norm	59,3	p_min_aut	53,4	p_min_aut	54,6
p_min_aut	61,0	sti_norm	47,7	sti_norm	54,7	p_min_aut	47,0	p_min_aut	47,0	p_min_aut	46,7	p_min_aut	50,5	p_min_aut	50,9	sti_norm	53,3	sti_norm	51,4
t_sd_aut	47,9	slope	39,8	t_sd_sum	35,1	slope	34,0	slope	34,6	slope	38,9	slope	36,9	t_sd_sum	45,4	t_sd_sum	42,6	t_sd_sum	34,9
t_sd_sum	46,3	spi_norm	38,8	slope	34,5	spi_norm	33,2	t_sd_sum	34,0	t_sd_aut	34,5	t_sd_sum	31,8	slope	31,8	slope	29,8		
slope	44,9	elev	33,5	spi_norm	32,7	p_max_win	32,6	t_sd_aut	33,4	t_sd_sum	30,8	spi_norm	29,0	spi_norm	31,6				
p_max_win	40,6	t_sd_sum	29,5	elev	29,7	t_sd_sum	29,4	spi_norm	33,0	spi_norm	28,5	t_sd_aut	26,8						
spi_norm	34,2	p_max_win	28,3	t_sd_aut	29,6	t_sd_aut	28,7	elev	28,2	elev	24,4								
elev	32,1	t_avg_aut	25,9	p_max_win	27,3	elev	25,9	p_max_win	27,0										
t_avg_aut	28,8	t_sd_aut	25,6	t_avg_aut	24,0	p_var_win	24,6	p_var_win	24,7										
p_var_win	28,4	p_var_win	23,2	p_var_win	21,7	t_avg_aut	24,6												
p_max_spr	27,7	p_max_spr	17,6	p_max_spr	16,1	p_max_spr	22,5												
p_min_spr	27,1	p_max_sum	16,0	p_min_win	13,3														
p_max_sum	25,1	p_min_win	14,3	p_max_sum	12,5														
p_var_spr	23,0	t_sd_win	12,2	t_sd_win	11,2														
t_sd_win	21,0	p_min_spr	11,2																
p_min_win	20,6	p_min_sum	10,4																
p_min_sum	20,2	p_var_spr	10,3																
p_avg_y	19,8	p_avg_y	10,0																
p_var_sum	18,2																		
p_max_aut	17,1																		
p_var_aut	16,3																		
t_min_sum	11,5																		
t_max_spr	11,3																		

importance (Table 2): 1) minimum precipitations during autumn (*p_min_aut*); 2) number of months within a normal range in temperatures (*sti_norm*); 3) variation in monthly temperatures during summer (*t_sd_sum*); and 4) *slope* (see **SI 4.** for detailed maps of these predictors).

3.2. GIs models

Based on model performance, we select *8var* as the final model for habitat suitability during GIs (Figs. 4 and 5). The VIF values indicate that the predictors retained exhibit a negligible degree of collinearity, with a value < 5 for each predictor.

The predictors included in the selected model are, in order of importance (Table 3): 1) variation in monthly temperatures in autumn (*t_sd_aut*); 2) maximum precipitations during winter (*p_max_win*); 3) *slope*; 4) maximum precipitations during spring (*p_max_spr*); 5) number of months within a normal range in temperatures (*sti_norm*); 6) seasonal variation in precipitations during spring (*p_var_spr*); 7) variation in monthly temperatures during winter (*t_sd_win*); and 8) variation in precipitation during winter (*p_var_win*) (see **SI 4.** for detailed maps of these predictors).

4. Discussion

4.1. Neanderthal habitat suitability in europe during MIS 3

RF relates the distribution of known occurrences (e.g., archaeological sites) with the environmental/spatial characteristics at those locations, producing a multi dimensional model that defines a set of suitable conditions for a given species. The model can be projected into geographical space and used to provide a better understanding of the environmental conditions a species prefers and/or to predict its potential geographic distribution., i.e., habitat suitability (Guisan and Zimmermann, 2000; Elith and Leathwick, 2009; Franklin et al., 2015). In general, habitat suitability produced values between 0 and 1: values tending towards 0 indicate a low potential habitat, values tending towards 1 indicate a high potential habitat (Kellner et al., 1992).

This research produced two habitat suitability maps for Neanderthal, considering GS and GI conditions in Europe during MIS 3 (Figs. 3 and 5). In addition to these two maps, we have also used a bar plot to compare the distribution of habitat suitability values in Europe for these two climatic phases (Fig. 6).

During GSs, habitat suitability values for much of Europe are low (0.3–0.4) and a relatively small proportion of the spatial domain has high habitat suitability values ($>$0.6) (Fig. 6). High values of habitat suitability are associated with six geographical areas: the Franco-Cantabrian region, southern Iberia, the east of the Paris basin, the Ardennes, the Rhone valley, and the Balkans (Fig. 3). These regions are separated from each other by what we can consider as paleoenvironmental boundaries, which can be identified in the center of Iberia, in the south of the Loire Valley, and in the south of the Alps. The territories in the north and northeast of the European area appear to be areas of low habitat suitability, most likely due to their proximity to the Scandinavian ice sheet and the continental Eurasian climate.

During GIs, in contrast, a proportionally larger territory has relatively high habitat suitability values ($>$0.6) and these are more evenly distributed across the territory, encompassing the geographical areas described for the GSs (Fig. 5). Medium to high values are also observed throughout the Paris Basin and are relatively more prevalent in Central and Eastern Europe. Northern Europe still has relatively low habitat suitability, likely related to the proximity of the Scandinavian ice cap and the continental Eurasian climate, which may have acted as paleoenvironmental and dispersal barriers from 55°N during the Pleistocene (Nielsen et al., 2017).

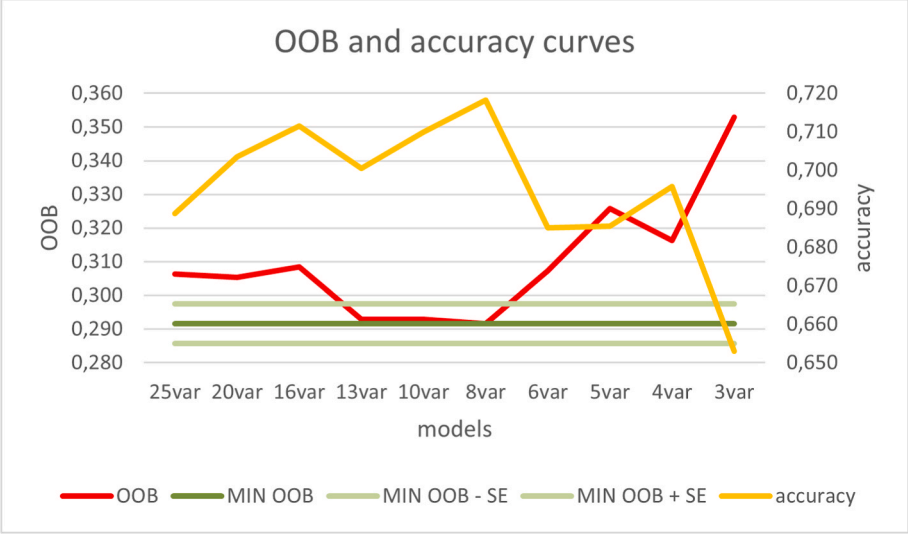

Fig. 4. Model performance indices for GIs models. OOB and accuracy values were extracted and averaged for each model run. The dark green line indicates the lowest OOB value (MIN = 0,2916), while the light green lines indicate one standard error from this value (SE = 0,0059). The results are rounded to the nearest 10e-4.

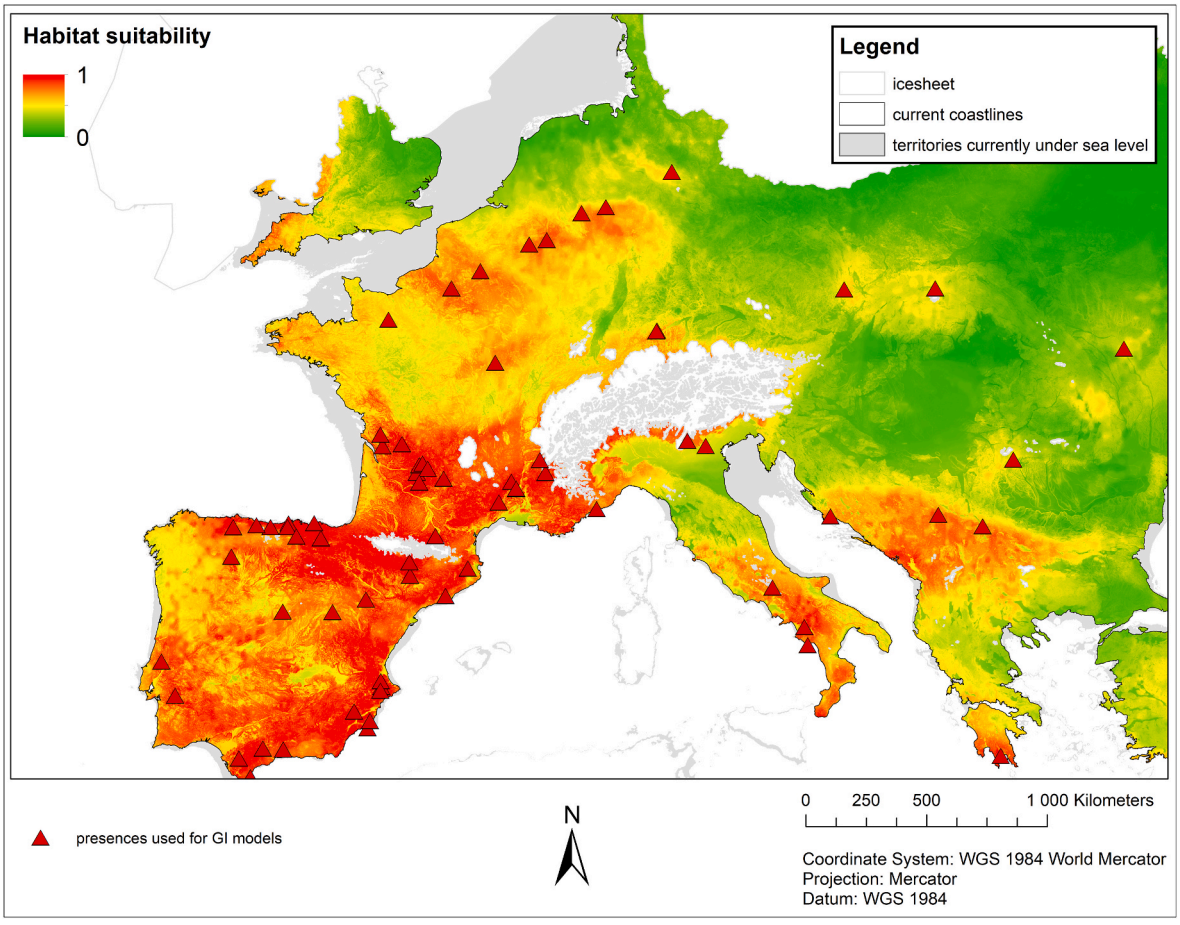

Fig. 5. Habitat suitability model for GIs. The habitat suitability model generated by the *8var* model and retained as the final model for GSs is displayed with the sites utilized as presences.

4.2. Significant predictors

The modeling methodology presented in this paper has allowed us to test two scales of climatic fluctuations that may have influenced the habitat suitability of Neanderthals in Europe during MIS 3: climate change and climate variability. Climate change refers to long-term, millennial fluctuations in global climate conditions that have affected the long-term evolutionary processes of our lineage (Potts, 1998; Grove, 2011) and influenced hominin dispersal (van Andel and Davies, 2003; Hublin and Roebroeks, 2009; Cupillard et al., 2013; Timmermann and

Table 3
Averaged Variable Importance (AVI) for GI models. Variable importance values were extracted and averaged for each model run and for each predictor. The results are rounded to the nearest 10e-1.

25var		20var		16var		13var		10var		8var		6var		5var		4var		3var	
t_sd_aut	63,6	p_max_win	62,9	p_max_win	61,8	t_sd_aut	63,2	t_sd_aut	63,3	t_sd_aut	67,4	t_sd_aut	64,2	p_max_win	59,6	p_max_win	59,5	p_max_win	59,2
p_max_win	60,7	t_sd_aut	58,1	t_sd_aut	60,5	p_max_win	59,7	p_max_win	58,6	p_max_win	59,8	p_max_win	62,5	t_sd_aut	59,3	t_sd_aut	58,4	t_sd_aut	53,5
slope	58,6	slope	56,5	slope	59,8	slope	47,0	slope	56,7	slope	50,1	slope	50,4	slope	48,0	slope	38,1	slope	31,2
sti_norm	28,1	t_sd_win	27,8	p_max_spr	26,9	p_max_spr	27,8	p_var_win	25,5	p_max_spr	25,4	p_max_spr	24,3	p_max_spr	24,8	p_max_spr	24,1		
t_sd_win	27,5	p_max_spr	26,2	p_var_spr	25,5	sti_norm	23,2	p_max_spr	24,2	sti_norm	23,1	sti_norm	18,2	sti_norm	15,4				
t_sd_sum	25,7	t_sd_sum	26,1	sti_norm	25,1	p_var_win	22,3	p_var_spr	23,7	p_var_spr	21,0	p_var_spr	15,1						
p_max_spr	25,6	p_var_win	25,6	p_max_sum	24,8	t_sd_sum	21,6	sti_norm	23,7	t_sd_win	18,3								
p_var_win	25,3	elev	24,5	t_sd_win	24,3	p_var_spr	21,3	t_sd_win	20,1	p_var_win	15,3								
p_max_aut	23,5	sti_norm	24,1	p_var_win	23,5	t_sd_win	20,8	p_max_aut	17,7										
p_max_sum	21,3	p_max_sum	22,0	t_sd_sum	23,0	p_max_aut	20,4	t_sd_sum	16,4										
elev	20,1	p_max_aut	21,0	elev	20,7	p_max_sum	20,3												
p_var_spr	17,7	p_var_spr	16,8	p_max_aut	19,1	p_min_sum	15,5												
spi_norm	17,5	p_min_sum	15,7	p_min_sum	18,8	elev	14,1												
p_min_sum	16,9	spi_norm	13,1	spi_norm	13,9														
t_avg_aut	12,7	p_min_aut	12,9	p_min_aut	11,8														
p_min_spr	11,8	t_avg_aut	12,6	t_avg_aut	10,3														
p_var_y	11,4	p_min_spr	11,1																
p_min_aut	10,6	p_var_y	10,2																
p_var_sum	10,5	p_var_sum	9,6																
p_min_win	8,6	p_min_win	4,7																
t_min_sum	6,6																		
p_var_aut	6,1																		
p_avg_y	5,9																		
t_max_spr	5,0																		
p_avg_sum	3,6																		

Friedrich, 2016; Timmermann et al., 2022). Climate variability refers to changes in climate conditions on smaller time scales compared to the mean climate trend and is also thought to have affected hominin evolution (Grove, 2011; Potts, 2013) and influenced human spatial behavior (Burke et al., 2017). Climate variability creates ecological risks, such as the periodic failure of key resources making foraging behavior uncertain (e.g., Winterhalder, 1986; Winterhalder et al., 1999; Kaplan, 2000).

The hypothesis that climate variability represents a form of risk that anatomically modern human (AMH) hunter-gatherers avoided was tested using RF in an earlier publication (Burke et al., 2017). Here, we test whether this hypothesis holds for Neanderthal populations using the same stepwise procedure and a set of candidate predictors designed to test whether or not climate variability is a key factor driving habitat suitability (for similar uses of RF, see: Genuer et al., 2010; Fox et al., 2017). The relative strength of the variables is quantified at each step and final model selection results in the identification of the best set of predictors. Several predictors associated with climate variability are selected for in our final models (Tables 2 and 3; Figs. 7 and 8), allowing us to conclude that Neanderthals, like AMHs (Paquin et al., 2024), avoid regions where climate variability is high. Our results also confirm the existence of shifts in the spatial behavior of Neanderthals under strongly contrasting stadial/interstadial climate regimes.

Relative to background values the response curves for the GS model (Fig. 7) indicate more predictable monthly temperatures (*sti_norm*) despite higher temperature variance in summer (*t_sd_sum*), higher precipitation minima in autumn (*p_min_aut*) and slightly higher slope values. This behavior suggests that Neanderthals avoided areas impacted by late drought, which may have resulted in a reduction of biomass richness and available resources prior to winter.

More predictable monthly temperatures are also indicated for GIs (Fig. 8) in addition to lower temperature variance in autumn and winter (*t_sd_aut*, *t_sd_win*), less variability in precipitation in spring and winter (*p_var_spr*, *p_var_win*), somewhat rainier than average conditions in winter (*p_max_win*) as opposed to spring (*p_max_spr*), and slightly higher slope values. These data suggest that less predictable environments were generally less suitable. We can conclude that Neanderthal groups tended to avoid regions where their ability to predict resource availability was limited. Slope values could reflect a preference for slightly more elevated positions above valley bottoms. Temperature maxima and minima did not emerge as significant predictors, indicating a tolerance for a range of temperature values while precipitation rates clearly more important determinants of habitat suitability.

4.3. *Characterizing neanderthal resilience*

Comparing the two habitat suitability models from a spatial and a chronological perspective helps evaluate preliminary hypotheses derived from our previous work (Albouy et al., 2023) about Neanderthal spatial behavior and resilience.

The temporal window between the GI-14 and GI-10, which encompasses the majority of documented sites, enables a more precise analysis of the demographic and population dynamics of Neanderthals between the GS and GI stages. Fig. 9 shows decreases and increases in the number of sites correlated with GS/GI cycles until GI-10, when the expected re-expansion of the Neanderthal population after GS-11 does not occur. The decreases in site numbers observed during GSs could be explained either by a population contraction, or the concentration of groups around fewer sites. Conversely, an increase in the number of sites during the GIs could indicate an increase in population size or a more dispersed territory exploitation strategy (see Albouy et al., 2023 for a discussion about GS/GI potential land use strategies). This pattern, sometimes described as “sinks and sources”, “ebb and flow” or “niche tracking” (see Hublin and Roebroeks, 2009; Dennell et al., 2011; Burke et al., 2017), is an indication of the resilience of Neanderthal populations during the Pleistocene as they recovered from climate downturns.

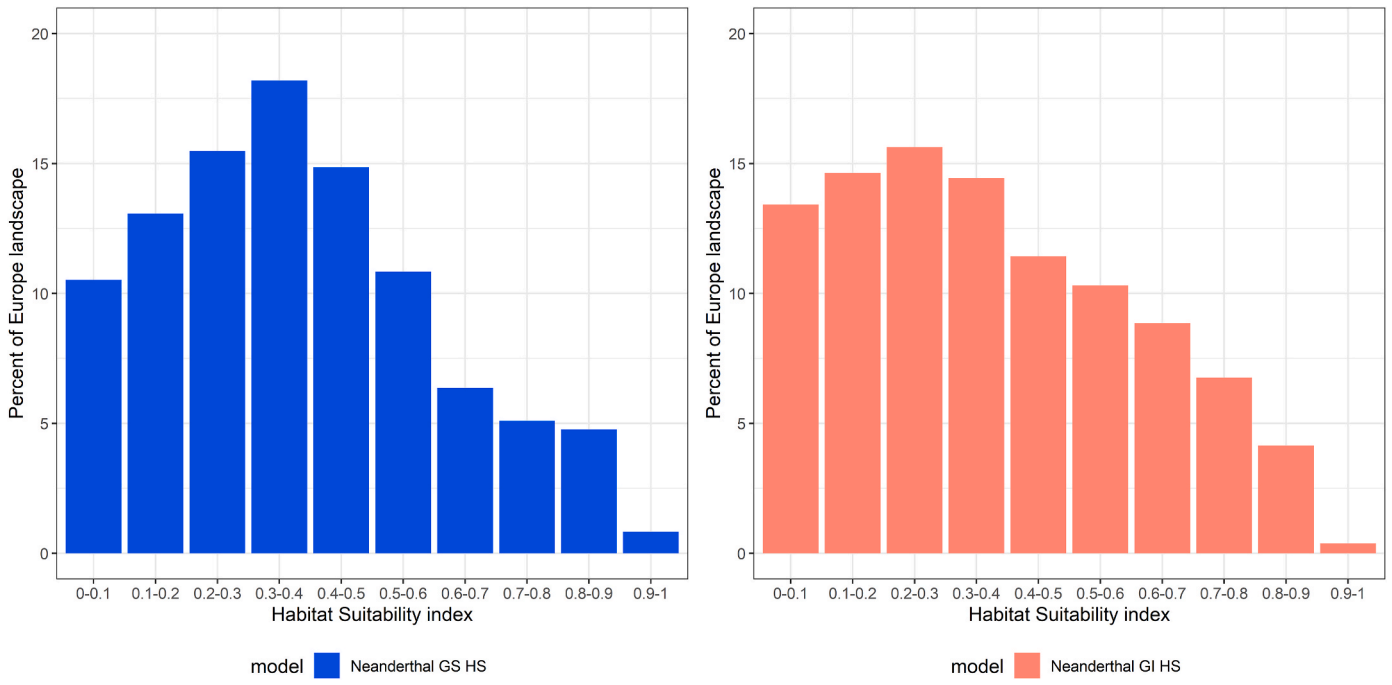

Fig. 6. Comparison of habitat suitability values representation in Europe between GSs and GIs. The bar plots illustrate the percentage of values within the European domain for each 0.1 habitat suitability interval. The blue bars represent values for the GIs model, while the red bars represent values for the GSs model.

Finally, it appears that GI-10, which coincided with Heinrich stadial 4 (HS-4) (Sánchez Goñi and Harrison, 2010), was a crucial period in Neanderthal population dynamics, marked by a failure to rebound after GS-11 and a significant decrease in recorded presences. The most recent sites recorded, i.e., Bajondillo for GS-10 and Cova Gran with Cueva del Boquete for GS-9, indicate the final retreat of the Neanderthal populations to what our model identifies as one of the "core" habitats, as suggested by previous studies (d'Errico and Sánchez Goñi, 2003; Finlayson, 2008; Jennings et al., 2011). This final contraction in the Iberian Peninsula may have been caused by the arrival of anatomically modern humans in Europe. Excluding potential early incursions, such as the Neronian (Slimak et al., 2022), the Aurignacian lithic techno-complex represents the first wave of permanent migration of *Homo sapiens* into Western Europe (Sawyer et al., 2015). Indeed, GI-10 marks a phase of significant population increase for this species in Europe (Paquin et al., 2023). It has been suggested that anatomically modern humans had greater tolerance for GS conditions (Staubwasser et al., 2018), facilitating their expansion through Europe (Vidal-Cordasco et al., 2022) at a time when Neanderthal populations contracted. This population shift may have resulted in the competitive exclusion of Neanderthals from favorable habitat at a time when they were undergoing climate-induced stress (Banks et al., 2008a; Melchionna, 2018; Melchionna et al., 2018; Timmermann, 2020; Klein et al., 2023).

4.4. Comparison with other published models

From a spatial perspective, when comparing the two habitat suitability models constructed in this work, we observe that during interstadials, the relative proportion of suitable territory was greater. The GIs, i.e., warm periods, were therefore more favorable for Neanderthals, providing room and resources for population expansion. Several authors have interpreted this as evidence for a Neanderthal preference for warmer conditions (Stewart, 2007; Serangeli and Bolus, 2008; Hublin and Roebroeks, 2009; Benito et al., 2017; Yaworsky et al., 2024). However, our results indicate that climate variability is more important than temperature in shaping Neanderthal habitat suitability. Regions that provide suitable habitat during both GSs and GIs could be considered core habitat. Our results confirm that southwestern Europe was a core habitat for Neanderthals during MIS 3 (van Andel and Davies, 2003; Serangeli and Bolus, 2008). As we suggested in a preliminary study (Albouy et al., 2023), it appears that the eastern portion of the Paris basin, the Ardennes and the Rhone Valley formed part of this core habitat. These areas of persistent settlement and retreat during the GSs can be considered as refuge areas (Bennett and Provan, 2008). Our models also identify three other, smaller core areas mentioned in the literature, including coastal areas (Finlayson, 2008): the Liguria (Finlayson, 2008; Riel-Salvatore et al., 2022), the Balkans and the Peloponnese (Finlayson, 2008). Finally, we confirm that the southern Iberian Peninsula represents the final retreat of Neanderthal populations prior to their extinction (d'Errico and Sánchez Goñi, 2003; Finlayson, 2008; Jennings et al., 2011).

The expansion of suitable habitat during the GIs implies a greater connectivity between populations occupying European space. Conversely, during the GS phases the fragmentation of habitable territory likely forced some Neanderthal groups to adapt quickly to unfavorable conditions (Bradtmöller et al., 2012) and eventually, abandon territory.

Previous research has also modeled the impact of MIS 3 climate fluctuations on the habitat of European Neanderthals (e.g., Banks et al., 2008a; Melchionna, 2018; Melchionna et al., 2018; Timmermann, 2020; Klein et al., 2023; Yaworsky et al., 2024). Although these studies differ from one another and from this research in terms of the presence data, climate simulations, candidate predictors, and modeling techniques, the resulting models are similar to ours.

In their pioneering work, Banks et al. (2008a) evaluated the extent of suitable habitat for Neanderthals during three MIS 3 phases: pre–HS–4 (GI-11 to GI-9), HS-4 and post–HS–4 (GI-8). Although their results cannot be directly compared to ours due to differences in chronology, their third model suggests a retreat of Neanderthals to southern Europe and the Iberian Peninsula, after HS-4.

More recently, Melchionna et al. (2018) used species distribution modeling to investigate the potential geographic ranges of Neanderthals at 48 ka BP, 44 ka BP, and 40 ka BP. The authors used presence data and four climatic predictors, including temperature and seasonal

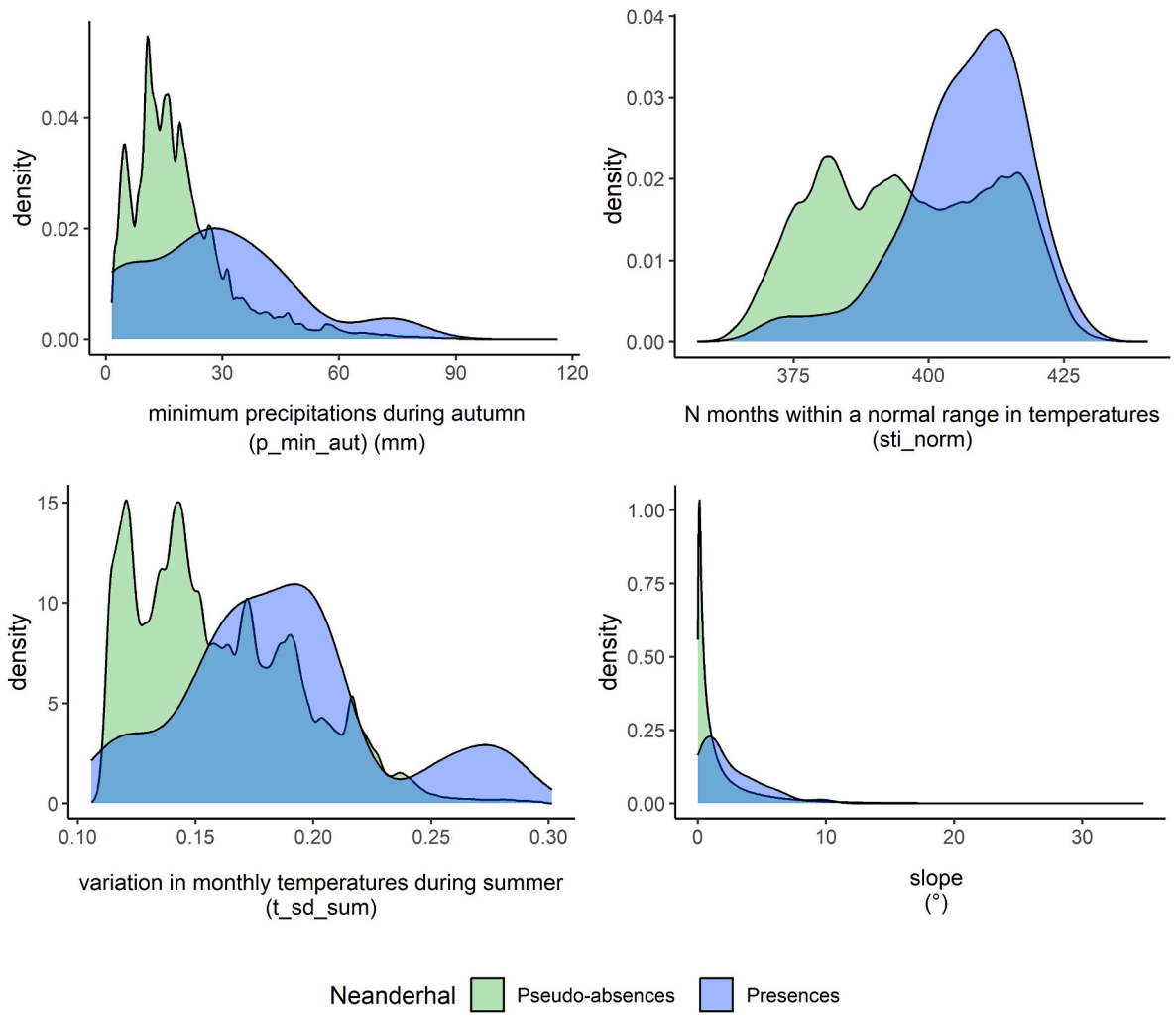

Fig. 7. Comparison of the predictors value density between presences and pseudoabsences used in GSs model. The density plots permit the comparison of the presence and pseudo-absence density for the predictor values included in the *4var* model. The predictors are presented in order of their averaged variable importance.

precipitation (winter and summer). They did not publish maps from their analyses. However, they identified a progressive reduction and fragmentation of the Neanderthal habitat during MIS 3, which is consistent with our observations.

Timmermann (2020) tests several hypotheses regarding the disappearance of the Neanderthals, including climate change (GS/GI) and the impact of interactions with *Homo sapiens* (interbreeding and competitive exclusion). Their results point out that climate fluctuations appear to have had only a minor impact on the Neanderthal extinction, with only regional effects. This suggests that the arrival of *Homo sapiens* in Europe may have disrupted Neanderthals' millennial repopulation strategies from their refuge areas, which is not incompatible with our results.

Klein et al. (2023) use logistic regression to model habitat suitability (Human Existence Potential) in the Iberian Peninsula for two climate phases: a warm phase (GI-11 to GI-10) and a cold phase (GS-10 to GS-9/HS-4). Their results indicate a high habitat potential in the coastal zones, as well as in the north and south of the peninsula, and a low habitat potential in the central region. They also observed a reduction and partitioning of suitable habitat during the cold phase. Our results show similar observations, but with less dispersion and heterogeneity of values. These differences can be partly explained by the fact that our research was conducted over a larger geographical area with a more limited choice of sites.

Another recent study, by Yaworsky et al. (2024), uses Maximum Entropy (MaxEnt) to explore Neanderthal niche space between 145 and 30 ka BP. Their results suggest a Neanderthal preference for warm climates. Therefore, the potential Neanderthal habitat in Europe would have been at its maximum during MIS 5e (121 ka BP). During MIS 3, their potential habitat expanded for the last time around 53 ka BP before finally shrinking until the species' extinction. Their models are consistent with ours and show an expansion of Neanderthals in MIS 3, concomitant to GI-14. In our results, however, it is only from GI-10 onwards that there appears to be a net population decline. It is possible that this difference can be partly explained by the fact that we use respectively different chronoclimatic scales. In any case, the observed population decline also seems to be linked to the arrival of *Homo sapiens*.

Our results are consistent with the main findings of previous studies and suggest that: 1) Neanderthal spatial behavior was affected by climate fluctuations during MIS 3; 2) habitat range expansions would have occurred during interstadial periods and contractions during stadial periods; and 3) the last Neanderthal populations are to be found in core habitat in the Iberian Peninsula, where they may have been relatively less exposed to competition with *Homo sapiens* dispersing from the East (Paquin et al., 2024). The differences observed between these studies and our research are partly explained by different modeling protocols. On the one hand, one of our explicit goals was to study the impact of climate change by contrasting habitat suitability models for GS and GIs. The classification of sites into GS and GI occupations also led us to be stricter in the number of sites selected (Albouy et al., 2023). We

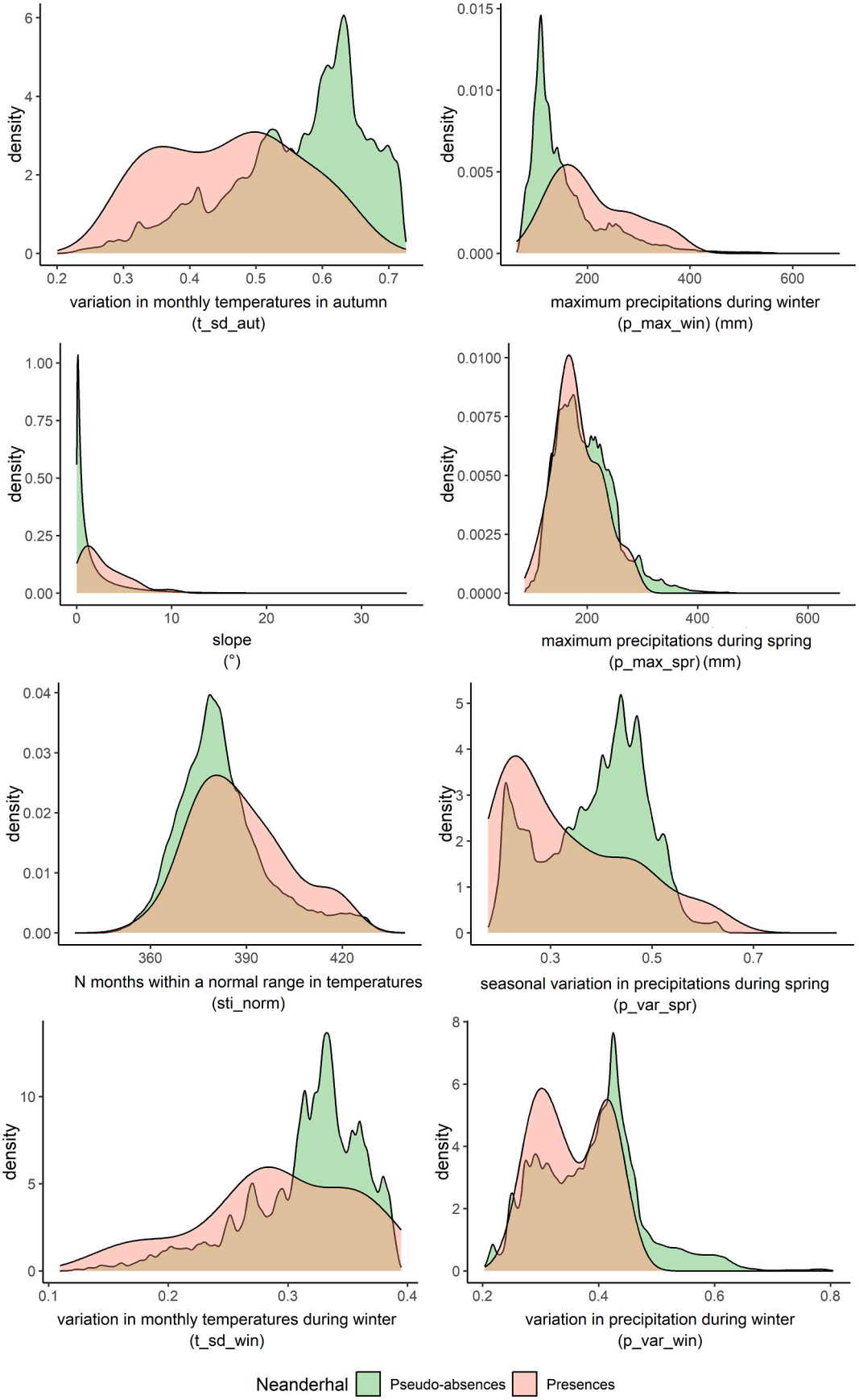

Fig. 8. Comparison of the predictors value density between presences and pseudoabsences used in GIs model. The density plots permit the comparison of the presence and pseudo-absence density for the predictor values included in the *8var* model. The predictors are presented in order of their averaged variable importance.

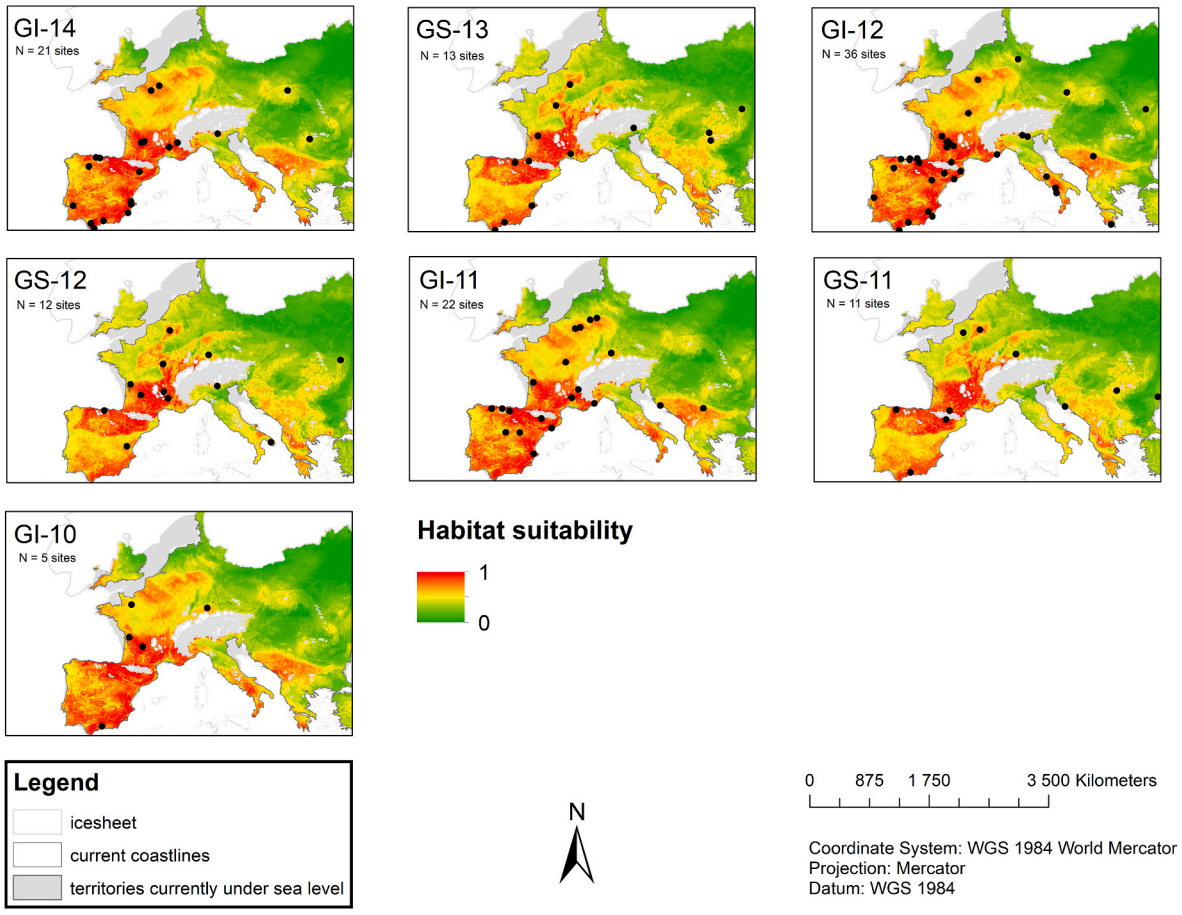

Fig. 9. Spatial and chronological distribution of Neanderthal in Europe during MIS 3. The sites utilized as presences were displayed on habitat suitability maps in order to provide an overview of Neanderthal demographic and population dynamics between the GS and GI climate phases. The temporal window selected is between the GI-14 and GI-10, which encompasses the majority of documented sites.

also explicitly chose to test predictors linked to climate variability, in addition to more conventional predictors such as temperature and precipitation averages and topographic variables.

5. Conclusion

The results of this research confirm that climate fluctuations affected the availability and distribution of suitable habitat for Neanderthal populations living in Europe during MIS 3. Furthermore, our findings indicate that southwest Europe constituted a core habitat for the species, in addition to several other smaller areas of persistent settlement which we refer to as refuge areas. These include the Liguria, the Balkans, the Peloponnese, and the Rhone valley. From a chronological perspective, we observed the reduction and fragmentation of suitable habitat during GSs and a re-expansion during GIs accompanied by decreases and increases in the number of sites that could indicate shifts in population size. Several of the climate predictors retained in our final models are associated with climate variability, suggesting that ecological risk management influenced Neanderthal spatial behavior during successive stadial/interstadial cycles of MIS 3. Re-expansions during GI events we interpret as evidence of climate resilience, until GI-10 which is marked by a significant decrease in recorded presences and a final population contraction in the Iberian Peninsula. This could be explained by the arrival of *Homo sapiens* in Europe, further taxing Neanderthal resilience and hampering their recovery.

Authors contributions

Benjamin Albouy: Conceptualization; Methodology; Formal Analysis; Visualization; Investigation; Writing – original draft; Data curation; Software. Simon Paquin: Investigation, Data curation; Methodology; Software. Julien Riel-Salvatore: Supervision, Writing – review & editing; Conceptualization. Masa Kageyama: Resources; Writing – review & editing; Software. Mathieu Vrac: Resources; Writing – review & editing; Software. Ariane Burke: Supervision, Writing – review & editing; Software; Conceptualization; Methodology; Funding Acquisition.

Declaration of competing interest

The authors declare that they have no known competing financial interests or personal relationships that could have appeared to influence the work reported in this paper.

Data availability

The climate simulations are available here: https://doi.org/10.5683/SP3/JBZQKS and the archaeological dataset here https://doi.org/10.5683/SP3/REV2IW.

Acknowledgments

This work was supported by the Fonds de Recherche du Québec Société et Culture [Project 2019-SE3-254686 and Project 316751]. We would also like to thank Marc Fasel and Martin Hinz for their help in

preparing the respective climate and archaeological data used in this work.

Appendix A. Supplementary data

Supplementary data to this article can be found online at https://doi.org/10.1016/j.quascirev.2024.108812.

References

Albouy, B., Paquin, S., Hinz, M., Wren, C.D., Burke, A., 2023. 2. The last of them. Investigating the paleogeography of the last Neanderthals in Europe (marine isotopic stage 3). In: Seuru, S., Albouy, B. (Eds.), Modelling Human-Environment Interactions in and beyond Prehistoric Europe, Themes in Contemporary Archaeology. Springer, Cham.

Banks, W.E., 2017. The application of ecological niche modeling methods to archaeological data in order to examine culture-environment relationships and cultural trajectories. Quat. Rev. Assoc. Fr. Pour Létude Quat. 28, 271–276. https://doi.org/10.4000/quaternaire.7966.

Banks, W.E., Aubry, T., d'Errico, F., Zilhão, J., Lira-Noriega, A., Townsend Peterson, A., 2011. Eco-cultural niches of the badegoulian: unraveling links between cultural adaptation and ecology during the last glacial maximum in France. J. Anthropol. Archaeol. 30, 359–374. https://doi.org/10.1016/j.jaa.2011.05.003.

Banks, W.E., d'Errico, F., Dibble, H.L., Krishtalka, L., West, D., Olszewski, D.I., Peterson, A.T., Anderson, D.G., Gillam, J.C., Montet-White, A., 2006. Eco-cultural niche modeling: new tools for reconstructing the geography and ecology of past human populations. PaleoAnthropology 4, 68–83.

Banks, W.E., d'Errico, F., Peterson, A.T., Kageyama, M., Sima, A., Sánchez-Goñi, M.-F., 2008a. Neanderthal extinction by competitive exclusion. PLoS One 3, e3972. https://doi.org/10.1371/journal.pone.0003972.

Banks, W.E., d'Errico, F., Peterson, A.T., Vanhaeren, M., Kageyama, M., Sepulchre, P., Ramstein, G., Jost, A., Lunt, D., 2008b. Human ecological niches and ranges during the LGM in Europe derived from an application of eco-cultural niche modeling. J. Archaeol. Sci. 35, 481–491. https://doi.org/10.1016/j.jas.2007.05.011.

Banks, W.E., d'Errico, F., Zilhão, J., 2013. Human–climate interaction during the early upper paleolithic: testing the hypothesis of an adaptive shift between the proto-aurignacian and the early aurignacian. J. Hum. Evol. 64, 39–55. https://doi.org/10.1016/j.jhevol.2012.10.001.

Banks, W.E., Moncel, M.-H., Raynal, J.-P., Cobos, M.E., Romero-Alvarez, D., Woillez, M.-N., Faivre, J.-P., Gravina, B., d'Errico, F., Locht, J.-L., Santos, F., 2021. An ecological niche shift for Neanderthal populations in Western Europe 70,000 years ago. Sci. Rep. 11, 5346. https://doi.org/10.1038/s41598-021-84805-6.

Barbet-Massin, M., Jiguet, F., Albert, C.H., Thuiller, W., 2012. Selecting pseudo-absences for species distribution models: how, where and how many? Methods Ecol. Evol. 3, 327–338. https://doi.org/10.1111/j.2041-210X.2011.00172.x.

Bennett, K.D., Provan, J., 2008. What do we mean by 'refugia'. Quaternary Science Reviews, Ice Age Refugia and Quaternary Extinctions: An Issue of Quaternary Evolutionary Palaeoecology 27, 2449–2455. https://doi.org/10.1016/j.quascirev.2008.08.019.

Benito, B.M., Svenning, J.-C., Kellberg-Nielsen, T., Riede, F., Gil-Romera, G., Mailund, T., Kjaergaard, P.C., Sandel, B.S., 2017. The ecological niche and distribution of Neanderthals during the Last Interglacial. J. Biogeogr. 44, 51–61. https://doi.org/10.1111/jbi.12845.

Braconnot, P., Harrison, S.P., Kageyama, M., Bartlein, P.J., Masson-Delmotte, V., Abe-Ouchi, A., Otto-Bliesner, B., Zhao, Y., 2012. Evaluation of climate models using palaeoclimatic data. Nat. Clim. Change 2, 417–424. https://doi.org/10.1038/nclimate1456.

Bradtmöller, M., Pastoors, A., Weninger, B., Weniger, G.-C., 2012. The repeated replacement model – rapid climate change and population dynamics in Late Pleistocene Europe. Quat. Int., The Neanderthal Home: spatial and social behaviours 247, 38–49. https://doi.org/10.1016/j.quaint.2010.10.015.

Breiman, L., 2001. Random forests. Mach. Learn. 45, 5–32. https://doi.org/10.1023/A:1010933404324.

Burjachs, F., López-García, J.M., Allué, E., Blain, H.-A., Rivals, F., Bennàsar, M., Expósito, I., 2012. Palaeoecology of Neanderthals during dansgaard–oeschger cycles in northeastern Iberia (abric romaní): from regional to global scale. Quat. Int., The Neanderthal Home: spatial and social behaviours 247, 26–37. https://doi.org/10.1016/j.quaint.2011.01.035.

Burke, A., 2000. Hunting in the middle palaeolithic. Int. J. Osteoarchaeol. 10, 281–285. https://doi.org/10.1002/1099-1212(200009/10)10:5<281::AID-OA568>3.0.CO;2-9.

Burke, A., Kageyama, M., Latombe, G., Fasel, M., Vrac, M., Ramstein, G., James, P.M.A., 2017. Risky business: the impact of climate and climate variability on human population dynamics in Western Europe during the Last Glacial Maximum. Quat. Sci. Rev. 164, 217–229. https://doi.org/10.1016/j.quascirev.2017.04.001.

Burke, A., Levavasseur, G., James, P.M.A., Guiducci, D., Izquierdo, M.A., Bourgeon, L., Kageyama, M., Ramstein, G., Vrac, M., 2014. Exploring the impact of climate variability during the Last Glacial Maximum on the pattern of human occupation of Iberia. J. Hum. Evol. 73, 35–46. https://doi.org/10.1016/j.jhevol.2014.06.003.

Burke, A., Riede, F., 2023. Conclusion. In: Seuru, S., Albouy, B. (Eds.), Modeling Human-Environment Interactions in and beyond Prehistoric Europe, Themes in Contemporary Archaeology. Springer, Cham.

Collard, M., Buchanan, B., Morin, J., Costopoulos, A., 2011. What drives the evolution of hunter–gatherer subsistence technology? A reanalysis of the risk hypothesis with data from the Pacific Northwest. Philos. Trans. R. Soc. B Biol. Sci. 366, 1129–1138. https://doi.org/10.1098/rstb.2010.0366.

Conard, N.J., Bolus, M., Münzel, S.C., 2012. Middle Paleolithic land use, spatial organization and settlement intensity in the Swabian Jura, southwestern Germany. Quat. Int., The Neanderthal Home: spatial and social behaviours 247, 236–245. https://doi.org/10.1016/j.quaint.2011.05.043.

Couronné, R., Probst, P., Boulesteix, A.-L., 2018. Random forest versus logistic regression: a large-scale benchmark experiment. BMC Bioinf. 19, 270. https://doi.org/10.1186/s12859-018-2264-5.

Cupillard, C., Malgarini, R., Fornage-Bontemps, S., 2013. Le Paléolithique supérieur ancien dans le quart nord-est de la France. Société Préhistorique Fr, LVI, 351–363.

Cutler, F., Wiener, R., 2022. randomForest: Breiman and Cutler's Random Forests for Classification and Regression.

d'Errico, F., Banks, W.E., Vanhaeren, M., Laroulandie, V., Langlais, M., 2011. PACEA geo-referenced radiocarbon database. PaleoAnthropology 2011, 1–12.

d'Errico, F., Sánchez Goñi, M.F., 2003. Neandertal extinction and the millennial scale climatic variability of OIS 3. Quat. Sci. Rev. 22, 769–788. https://doi.org/10.1016/S0277-3791(03)00009-X.

d'Errico, F., Zilhão, J., Julien, M., Baffier, D., Pelegrin, J., 1998. Neanderthal acculturation in western Europe? A critical review of the evidence and its interpretation. Curr. Anthropol. 39, S1–S44. https://doi.org/10.1086/204689.

Dansgaard, W., Johnsen, S.J., Clausen, H.B., Dahl-Jensen, D., Gundestrup, N., Hammer, C.U., Oeschger, H., 1984. North atlantic climatic oscillations revealed by deep Greenland ice cores. Am. Geophys. Union 29, 288–298. https://doi.org/10.1029/GM029p0288.

Dansgaard, W., Johnsen, S.J., Clausen, H.B., Dahl-Jensen, D., Gundestrup, N.S., Hammer, C.U., Hvidberg, C.S., Steffensen, J.P., Sveinbjörnsdottir, A.E., Jouzel, J., Bond, G., 1993. Evidence for general instability of past climate from a 250-kyr ice-core record. Nature 364, 218–220. https://doi.org/10.1038/364218a0.

Daujeard, C., Fernandes, P., Guadelli, J.-L., Moncel, M.-H., Santagata, C., Raynal, J.-P., 2012. Neanderthal subsistence strategies in southeastern France between the plains of the Rhone Valley and the mid-mountains of the massif central (MIS 7 to MIS 3). Quat. Int., The evolution of the hominin food resource exploitation in Pleistocene Europe: Recent Studies in Zooarchaeology 252, 32–47. https://doi.org/10.1016/j.quaint.2011.01.047.

Delagnes, A., Jaubert, J., Meignen, L., 2007. Les technocomplexes du Paléolithique moyen en Europe occidentale dans leur cadre diachronique et géographique. In: Vandermeersch, B., Maureille, B. (Eds.), Les Néandertaliens. Biologie et Cultures. Editions du CTHS, pp. 213–229.

Delagnes, A., Rendu, W., 2011. Shifts in Neandertal mobility, technology and subsistence strategies in western France. J. Archaeol. Sci. 38, 1771–1783. https://doi.org/10.1016/j.jas.2011.04.007.

Dennell, R.W., Martinón-Torres, M., Bermúdez de Castro, J.M., 2011. Hominin variability, climatic instability and population demography in Middle Pleistocene Europe. Quat. Sci. Rev., Early Human Evolution in the Western Palaearctic: Ecological Scenarios 30, 1511–1524. https://doi.org/10.1016/j.quascirev.2009.11.027.

Devièse, T., Abrams, G., Hajdinjak, M., Pirson, S., Groote, I.D., Modica, K.D., Toussaint, M., Fischer, V., Comeskey, D., Spindler, L., Meyer, M., Semal, P., Higham, T., 2021. Reevaluating the timing of neanderthal disappearance in northwest Europe. Proc. Natl. Acad. Sci. USA 118. https://doi.org/10.1073/pnas.2022466118.

Díaz-Uriarte, R., Alvarez de Andrés, S., 2006. Gene selection and classification of microarray data using random forest. BMC Bioinf. 7, 1–13. https://doi.org/10.1186/1471-2105-7-3.

Dufresne, J.-L., Foujols, M.-A., Denvil, S., Caubel, A., Marti, O., Aumont, O., Balkanski, Y., Bekki, S., Bellenger, H., Benshila, R., Bony, S., Bopp, L., Braconnot, P., Brockmann, P., Cadule, P., Cheruy, F., Codron, F., Cozic, A., Cugnet, D., de Noblet, N., Duvel, J.-P., Ethé, C., Fairhead, L., Fichefet, T., Flavoni, S., Friedlingstein, P., Grandpeix, J.-Y., Guez, L., Guilyardi, E., Hauglustaine, D., Hourdin, F., Idelkadi, A., Ghattas, J., Joussaume, S., Kageyama, M., Krinner, G., Labetoulle, S., Lahellec, A., Lefebvre, M.-P., Lefevre, F., Levy, C., Li, Z.X., Lloyd, J., Lott, F., Madec, G., Mancip, M., Marchand, M., Masson, S., Meurdesoif, Y., Mignot, J., Musat, I., Parouty, S., Polcher, J., Rio, C., Schulz, M., Swingedouw, D., Szopa, S., Talandier, C., Terray, P., Viovy, N., Vuichard, N., 2013. Climate change projections using the IPSL-CM5 earth system model: from CMIP3 to CMIP5. Clim. Dynam. 40, 2123–2165. https://doi.org/10.1007/s00382-012-1636-1.

Ehlers, J., Ehlers, Jürgen, Gibbard, P.L., Hughes, P.D., 2011. Quaternary Glaciations - Extent and Chronology: A Closer Look. Elsevier.

Elith, J., Leathwick, J.R., 2009. Species distribution models: ecological explanation and prediction across space and time. Annu. Rev. Ecol. Evol. Systemat. 40, 677–697. https://doi.org/10.1146/annurev.ecolsys.110308.120159.

Ember, C.R., Ember, M., 1992. Resource unpredictability, mistrust, and war: a cross-cultural study. J. Conflict Resolut. 36, 242–262. https://doi.org/10.1177/0022002792036002002.

Fasel, M., 2015. STI: Calculation of the Standardized Temperature Index.

Fernàndez-Laso, M.C., Rivals, F., Rosell, J., 2010. Intra-site changes in seasonality and their consequences on the faunal assemblages from Abric Romanf (Middle Palaeolithic, Spain). Quat. Rev. Assoc. Fr. Pour Létude Quat. 21, 155–163. https://doi.org/10.4000/quaternaire.5525.

Finlayson, C., Fa, D.A., Jiménez Espejo, F., Carrión, J.S., Finlayson, G., Giles Pacheco, F., Rodríguez Vidal, J., Stringer, C., Martínez Ruiz, F., 2008. Gorham's Cave, Gibraltar—the persistence of a Neanderthal population. Quaternary International,

The Last 15ka of Environmental Change in Mediterranean Regions - Interpreting Different Archives 181, 64–71. https://doi.org/10.1016/j.quaint.2007.11.016.
Fiorenza, L., Benazzi, S., Henry, A.G., Salazar-García, D.C., Blasco, R., Picin, A., Wroe, S., Kullmer, O., 2015. To meat or not to meat? New perspectives on Neanderthal ecology. Am. J. Phys. Anthropol. 156, 43–71. https://doi.org/10.1002/ajpa.22659.
Fox, E.W., Hill, R.A., Leibowitz, S.G., Olsen, A.R., Thornbrugh, D.J., Weber, M.H., 2017. Assessing the accuracy and stability of variable selection methods for random forest modeling in ecology. Environ. Monit. Assess. 189, 316. https://doi.org/10.1007/s10661-017-6025-0.
Franklin, J., Potts, A.J., Fisher, E.C., Cowling, R.M., Marean, C.W., 2015. Paleodistribution modeling in archaeology and paleoanthropology. Quat. Sci. Rev. 110, 1–14. https://doi.org/10.1016/j.quascirev.2014.12.015.
Genuer, R., Poggi, J.-M., Tuleau-Malot, C., 2010. Variable selection using random forests. Pattern Recogn. Lett. 31, 2225–2236. https://doi.org/10.1016/j.patrec.2010.03.014.
Grömping, U., 2009. Variable importance assessment in regression: linear regression versus random forest. Am. Statistician 63, 308–319. https://doi.org/10.1198/tast.2009.08199.
Grove, M., 2011. Change and variability in Plio-Pleistocene climates: modelling the hominin response. J. Archaeol. Sci. 38, 3038–3047. https://doi.org/10.1016/j.jas.2011.07.002.
Guisan, A., Zimmermann, N.E., 2000. Predictive habitat distribution models in ecology. Ecol. Model. 135, 147–186. https://doi.org/10.1016/S0304-3800(00)00354-9.
Guttman, N.B., 1999. Accepting the standardized precipitation index: a calculation Algorithm1. JAWRA J. Am. Water Resour. Assoc. 35, 311–322. https://doi.org/10.1111/j.1752-1688.1999.tb03592.x.
Hayes, M., 2000. Revisiting the SPI: clarifying the process. Drought Netw. News 1994-2001 18.
Heinrich, H., 1988. Origin and consequences of cyclic ice rafting in the Northeast Atlantic Ocean during the past 130,000 years. Quat. Res. 29, 142–152. https://doi.org/10.1016/0033-5894(88)90057-9.
Heydari-Guran, S., Benazzi, S., Talamo, S., Ghasidian, E., Hariri, N., Oxilia, G., Asiabani, S., Azizi, F., Naderi, R., Safaierad, R., Hublin, J.-J., Foley, R.A., Lahr, M.M., 2021. The discovery of an in situ neanderthal remain in the bawa yawan rockshelter, west-central zagros mountains, kermanshah. PLoS One 16, e0253708. https://doi.org/10.1371/journal.pone.0253708.
Higham, T.F.G., Douka, K., Wood, R., Bronk Ramsey, C., Brock, F., Basell, L., Camps, M., Arrizabalaga, A., Baena, J., Barroso-Ruíz, C., Bergman, C., Boitard, C., Boscato, P., Caparrós, M., Conard, N.J., Draily, C., Froment, A., Galván, B., Gambassini, P., Garcia-Moreno, A., Grimaldi, S., Haesaerts, P., Holt, B., Iriarte-Chiapusso, M.-J., Jelinek, A., Jordá Pardo, J.F., Maíllo-Fernández, J.-M., Marom, A., Maroto, J., Menéndez, M., Metz, L., Morin, E., Moroni, A., Negrino, F., Panagopoulou, E., Peresani, M., Pirson, S., de la Rasilla, M., Riel-Salvatore, J., Ronchitelli, A., Santamaria, D., Semal, P., Slimak, L., Soler, J., Soler, N., Villaluenga, A., Pinhasi, R., Jacobi, R., 2014. The timing and spatiotemporal patterning of Neanderthal disappearance. Nature 512, 306–309. https://doi.org/10.1038/nature13621.
Hublin, J.-J., 2015. The modern human colonization of western Eurasia: when and where? Quat. Sci. Rev., Synchronising Environmental and Archaeological Records using Volcanic Ash Isochrons 118, 194–210. https://doi.org/10.1016/j.quascirev.2014.08.011.
Hublin, J.-J., 2009. The origin of Neandertals. Proc. Natl. Acad. Sci. U.S.A. 106, 16022–16027. https://doi.org/10.1073/pnas.0904119106.
Hublin, J.-J., Roebroeks, W., 2009. Ebb and flow or regional extinctions? On the character of Neandertal occupation of northern environments. Comptes Rendus Palevol 8, 503–509. https://doi.org/10.1016/j.crpv.2009.04.001.
Jennings, R., Finlayson, C., Fa, D., Finlayson, G., 2011. Southern Iberia as a refuge for the last Neanderthal populations. J. Biogeogr. 38, 1873–1885. https://doi.org/10.1111/j.1365-2699.2011.02536.x.
Kageyama, M., Braconnot, P., Bopp, L., Caubel, A., Foujols, M.-A., Guilyardi, E., Khodri, M., Lloyd, J., Lombard, F., Mariotti, V., Marti, O., Roy, T., Woillez, M.-N., 2013. Mid-Holocene and Last Glacial Maximum climate simulations with the IPSL model—part I: comparing IPSL_CM5A to IPSL_CM4. Clim. Dynam. 40, 2447–2468. https://doi.org/10.1007/s00382-012-1488-8.
Kaplan, D., 2000. The darker side of the "original affluent society.". J. Anthropol. Res. 56, 301–324. https://doi.org/10.1086/jar.56.3.3631086.
Kearney, M., 2006. Habitat, environment and niche: what are we modelling? Oikos 115, 186–191. https://doi.org/10.1111/j.2006.0030-1299.14908.x.
Kellner, C.J., Brawn, J.D., Karr, J.R., 1992. What is habitat suitability and how should it be measured? In: McCullough, D.R., Barrett, R.H. (Eds.), Wildlife 2001: Populations. Springer, Netherlands, Dordrecht, pp. 476–488. https://doi.org/10.1007/978-94-011-2868-1_36.
Kelly, R.L., 2013. The Lifeways of Hunter-Gatherers: the Foraging Spectrum. Cambridge University Press, Cambridge. https://doi.org/10.1017/CBO9781139176132.
Klein, K., Weniger, G.-C., Ludwig, P., Stepanek, C., Zhang, X., Wegener, C., Shao, Y., 2023. Assessing climatic impact on transition from Neanderthal to anatomically modern human population on Iberian Peninsula: a macroscopic perspective. Sci. Bull. https://doi.org/10.1016/j.scib.2023.04.025.
Kuhn, M., Wing, J., Weston, S., Williams, A., Keefer, C., Engelhardt, A., Cooper, T., Mayer, Z., Kenkel, B., R Core Team, Benesty, M., Lescarbeau, R., Ziem, A., Scrucca, L., Tang, Y., Candan, C., Hunt, T., 2022. Caret: Classification and Regression Training.
Latombe, G., Burke, A., Vrac, M., Levavasseur, G., Dumas, C., Kageyama, M., Ramstein, G., 2018. Comparison of spatial downscaling methods of general circulation model results to study climate variability during the Last Glacial Maximum. Geosci. Model Deviat 11, 2563–2579. https://doi.org/10.5194/gmd-11-2563-2018.
Liaw, A., Wiener, M., 2002. Classification and regression by randomForest. R. News 2, 18–22.
Ludwig, P., Shao, Y., Kehl, M., Weniger, G.-C., 2018. The Last Glacial Maximum and Heinrich event I on the Iberian Peninsula: a regional climate modelling study for understanding human settlement patterns. Global Planet. Change 170, 34–47. https://doi.org/10.1016/j.gloplacha.2018.08.006.
Martínez, K., García, J., Chacón, M.G., Fernández-Laso, M.C., 2005. Le Paléolithique moyen de l'Abric Romaní. Comportements écosociaux des groupes néandertaliens. L'Anthropologie 109, 815–839. https://doi.org/10.1016/j.anthro.2005.10.001.
McKee, T.B., Doesken, N.J., Kleist, J., 1993. The relationship of drought frequency and duration to time scales. In: Presented at the 8th Conference on Applied Climatology, Anaheim, 17-22 January 1993, pp. 179–184. Anaheim, California.
Melchionna, M., 2018. Small and isolated: ecology and fragmentation of Neanderthals. Foss. - Rep. Palaeontol 53–56.
Melchionna, M., Di Febbraro, M., Carotenuto, F., Rook, L., Mondanaro, A., Castiglione, S., Serio, C., Vero, V.A., Tesone, G., Piccolo, M., Diniz-Filho, J.A.F., Raia, P., 2018. Fragmentation of Neanderthals' pre-extinction distribution by climate change. Palaeogeogr. Palaeoclimatol. Palaeoecol. 496, 146–154. https://doi.org/10.1016/j.palaeo.2018.01.031.
Nielsen, T.K., Benito, B.M., Svenning, J.-C., Sandel, B., McKerracher, L., Riede, F., Kjærgaard, P.C., 2017. Investigating neanderthal dispersal above 55°N in Europe during the last interglacial complex. Quaternary International, Pleistocene human dispersals: Climate, ecology and social behavior 431, 88–103. https://doi.org/10.1016/j.quaint.2015.10.039.
Ordonez, A., Riede, F., 2022. Changes in limiting factors for forager population dynamics in Europe across the last glacial-interglacial transition. Nat. Commun. 13, 5140. https://doi.org/10.1038/s41467-022-32750-x.
Paquin, S., Albouy, B., Hinz, M., Burke, A., 2023. 3. Going new places: dispersal and establishment of the aurignacian technocomplex in Europe during the marine isotopic stage 3 (MIS 3). In: Seuru, S., Albouy, B. (Eds.), Modeling Human-Environment Interactions in and beyond Prehistoric Europe, Themes in Contemporary Archaeology. Springer, Cham.
Paquin, S., Albouy, B., Kageyama, M., Vrac, M., Burke, A., 2024. Anatomically modern human dispersals into Europe during MIS 3: climate stability, paleogeography and habitat suitability. Quat. Sci. Rev. 330, 108596 https://doi.org/10.1016/j.quascirev.2024.108596.
Patou-Mathis, M., 2000. Neanderthal subsistence behaviours in Europe. Int. J. Osteoarchaeol. 10, 379–395. https://doi.org/10.1002/1099-1212(200009/10)10:5<379::AID-OA558>3.0.CO;2-4.
Pettitt, P.B., Davies, W., Gamble, C.S., Richards, M.B., 2003. Palaeolithic radiocarbon chronology: quantifying our confidence beyond two half-lives. J. Archaeol. Sci. 30, 1685–1693. https://doi.org/10.1016/S0305-4403(03)00070-0.
Potts, R., 2013. Hominin evolution in settings of strong environmental variability. Quat. Sci. Rev. 73, 1–13. https://doi.org/10.1016/j.quascirev.2013.04.003.
Potts, R., 1998. Environmental hypotheses of hominin evolution. Am. J. Phys. Anthropol. 107, 93–136. https://doi.org/10.1002/(SICI)1096-8644(1998)107:27+<93::AID-AJPA5>3.0.CO;2-X.
R Core Team, 2024. R: A Language and Environment for Statistical Computing. R Foundation for Statistical Computing, Vienna, Austria.
Rasmussen, S.O., Bigler, M., Blockley, S.P., Blunier, T., Buchardt, S.L., Clausen, H.B., Cvijanovic, I., Dahl-Jensen, D., Johnsen, S.J., Fischer, H., Gkinis, V., Guillevic, M., Hoek, W.Z., Lowe, J.J., Pedro, J.B., Popp, T., Seierstad, I.K., Steffensen, J.P., Svensson, A.M., Vallelonga, P., Vinther, B.M., Walker, M.J.C., Wheatley, J.J., Winstrup, M., 2014. A stratigraphic framework for abrupt climatic changes during the Last Glacial period based on three synchronized Greenland ice-core records: refining and extending the INTIMATE event stratigraphy. Quat. Sci. Rev. 106, 14–28. https://doi.org/10.1016/j.quascirev.2014.09.007. Dating, Synthesis, and Interpretation of Palaeoclimatic Records and Model-data Integration: Advances of the INTIMATE project (INTegration of Ice core, Marine and TErrestrial records, COST Action ES0907).
Rendu, W., 2007. Planification des activités de subsistance au sein du territoire des derniers Moustériens Cémentochronologie et approche archéozoologique de gisements du Paléolithique moyen (Pech-de-l'Azé I, La Quina, Mauran) et Paléolithique supérieur ancien (Isturitz) (phdthesis). Université Bordeaux 1.
Rendu, W., Beauval, C., Crevecoeur, I., Bayle, P., Balzeau, A., Bismuth, T., Bourguignon, L., Delfour, G., Faivre, J.-P., Lacrampe-Cuyaubère, F., Tavormina, C., Todisco, D., Turq, A., Maureille, B., 2014. Evidence supporting an intentional Neandertal burial at La Chapelle-aux-Saints. Proc. Natl. Acad. Sci. USA 111, 81–86. https://doi.org/10.1073/pnas.1316780110.
Rendu, W., Costamagno, S., Meignen, L., Soulier, M.-C., 2012. Monospecific faunal spectra in Mousterian contexts: implications for social behavior. Quat. Int., The Neanderthal Home: spatial and social behaviours 247, 50–58. https://doi.org/10.1016/j.quaint.2011.01.022.
Riel-Salvatore, J., Ludeke, I.C., Negrino, F., Holt, B.M., 2013. A spatial analysis of the late mousterian levels of riparo bombrini (balzi rossi, Italy). Can. J. Archaeol. J. Can. Archéologie 37, 70–92.
Riel-Salvatore, J., Negrino, F., Pothier Bouchard, G., Vallerand, A., Costa, S., Benazzi, S., 2022. The 'semi-sterile mousterian' of riparo bombrini: evidence of a late-lasting neanderthal refugium in Liguria. J. Quat. Sci. 37, 268–282. https://doi.org/10.1002/jqs.3411.
Roebroeks, W., Soressi, M., 2016. Neandertals revised. Proc. Natl. Acad. Sci. USA 113, 6372–6379. https://doi.org/10.1073/pnas.1521269113.
RStudio Team, 2023. RStudio. integrated development for R. RStudio, PBC, Boston, MA.
Sánchez Goñi, M.F., Harrison, S.P., 2010. Millennial-scale climate variability and vegetation changes during the Last Glacial: concepts and terminology. Quat. Sci.

Rev., Vegetation Response to Millennial-scale Variability during the Last Glacial 29, 2823–2827. https://doi.org/10.1016/j.quascirev.2009.11.014.
Sawyer, S., Renaud, G., Viola, B., Hublin, J.-J., Gansauge, M.-T., Shunkov, M.V., Derevianko, A.P., Prüfer, K., Kelso, J., Pääbo, S., 2015. Nuclear and mitochondrial DNA sequences from two Denisovan individuals. Proc. Natl. Acad. Sci. USA 112, 15696–15700. https://doi.org/10.1073/pnas.1519905112.
Schmidt, I., Bradtmöller, M., Kehl, M., Pastoors, A., Tafelmaier, Y., Weninger, B., Weniger, G.-C., 2012. Rapid climate change and variability of settlement patterns in Iberia during the late pleistocene. Quat. Int., Temporal and Spatial Corridors of Homo Sapiens Sapiens Population dynamics during the Late Pleistocene and Early Holocene 274, 179–204. https://doi.org/10.1016/j.quaint.2012.01.018.
Sepulchre, P., Ramstein, G., Kageyama, M., Vanhaeren, M., Krinner, G., Sánchez-Goñi, M.-F., d'Errico, F., 2007. H4 abrupt event and late Neanderthal presence in Iberia. Earth Planet Sci. Lett. 258, 283–292. https://doi.org/10.1016/j.epsl.2007.03.041.
Serangeli, J., Bolus, M., 2008. Out of Europe-The dispersal of a successful European hominin form. Quartar 55, 83–98.
Slimak, L., Zanolli, C., Higham, T., Frouin, M., Schwenninger, J.-L., Arnold, L.J., Demuro, M., Douka, K., Mercier, N., Guérin, G., Valladas, H., Yvorra, P., Giraud, Y., Seguin-Orlando, A., Orlando, L., Lewis, J.E., Muth, X., Camus, H., Vandevelde, S., Buckley, M., Mallol, C., Stringer, C., Metz, L., 2022. Modern human incursion into Neanderthal territories 54,000 years ago at Mandrin, France. Sci. Adv. 8, eabj9496 https://doi.org/10.1126/sciadv.abj9496.
Soressi, M., d'Errico, F., 2007. Pigments, gravures, parures : les comportements symboliques controversés des Néandertaliens. In: B, Vandermeersch, B.M. (Eds.), Les Néandertaliens. Biologie et Cultures, Documents Préhistoriques 23. Éditions du CTHS, pp. 297–309.
Staubwasser, M., Drăgușin, V., Onac, B.P., Assonov, S., Ersek, V., Hoffmann, D.L., Veres, D., 2018. Impact of climate change on the transition of Neanderthals to modern humans in Europe. Proc. Natl. Acad. Sci. USA 115, 9116–9121. https://doi.org/10.1073/pnas.1808647115.
Stewart, J.R., 2007. Neanderthal extinction as part of the faunal change in Europe during oxygen Isotope stage 3. Acta Zool. Cracoviensia - Ser. A Vertebr. 50, 93–124. https://doi.org/10.3409/000000007783995372.
Svensson, A., Andersen, K.K., Bigler, M., Clausen, H.B., Dahl-Jensen, D., Davies, S.M., Johnsen, S.J., Muscheler, R., Parrenin, F., Rasmussen, S.O., Röthlisberger, R., Seierstad, I., Steffensen, J.P., Vinther, B.M., 2008. A 60 000 year Greenland stratigraphic ice core chronology. Clim. Past 4, 47–57. https://doi.org/10.5194/cp-4-47-2008.
Svensson, A., Andersen, K.K., Bigler, M., Clausen, H.B., Dahl-Jensen, D., Davies, S.M., Johnsen, S.J., Muscheler, R., Rasmussen, S.O., Röthlisberger, R., Peder Steffensen, J., Vinther, BoM., 2006. The Greenland Ice Core Chronology 2005, 15–42ka. Part 2: comparison to other records. Quaternary Science Reviews, Critical Quaternary Stratigraphy 25, 3258–3267. https://doi.org/10.1016/j.quascirev.2006.08.003.
Tallavaara, M., Luoto, M., Korhonen, N., Järvinen, H., Seppä, H., 2015. Human population dynamics in Europe over the last glacial maximum. Proc. Natl. Acad. Sci. USA 112, 8232–8237. https://doi.org/10.1073/pnas.1503784112.
Timmermann, A., 2020. Quantifying the potential causes of Neanderthal extinction: abrupt climate change versus competition and interbreeding. Quat. Sci. Rev. 238, 106331 https://doi.org/10.1016/j.quascirev.2020.106331.
Timmermann, A., Friedrich, T., 2016. Late Pleistocene climate drivers of early human migration. Nature 538, 92–95. https://doi.org/10.1038/nature19365.
Timmermann, A., Yun, K.-S., Raia, P., Ruan, J., Mondanaro, A., Zeller, E., Zollikofer, C., Ponce de León, M., Lemmon, D., Willeit, M., Ganopolski, A., 2022. Climate effects on archaic human habitats and species successions. Nature 1–7. https://doi.org/10.1038/s41586-022-04600-9.
Vallverdú, J., Allué, E., Bischoff, J.L., Cáceres, I., Carbonell, E., Cebrià, A., García-Antón, D., Huguet, R., Ibáñez, N., Martínez, K., Pastó, I., Rosell, J., Saladié, P., Vaquero, M., 2005. Short human occupations in the middle palaeolithic level i of the abric romaní rock-shelter (capellades, barcelona, Spain). J. Hum. Evol. 48, 157–174. https://doi.org/10.1016/j.jhevol.2004.10.004.
van Andel, T.H., Davies, W. (Eds.), 2003. Neanderthals and Modern Humans in the European Landscape during the Last Glaciation: Archaeological Results of the Stage 3 Project. McDonald Institute monographs. McDonald Institute for Archaeological Research ; Distributed by Oxbow Books, Cambridge : Oxford.
Vermeersch, P.M., 2019. Radiocarbon palaeolithic europe database V20. JUNE 2019 [WWW Document]. URL. https://ees.kuleuven.be/geography/projects/14c-palaeolithic/index.html. accessed 1.29.20.
Vicente-Serrano, S.M., Beguería, S., López-Moreno, J.I., 2010. A multiscalar drought index sensitive to global warming: the standardized precipitation evapotranspiration index. J. Clim. 23, 1696–1718. https://doi.org/10.1175/2009JCLI2909.1.
Vidal-Cordasco, M., Ocio, D., Hickler, T., Marín-Arroyo, A.B., 2022. Ecosystem productivity affected the spatiotemporal disappearance of Neanderthals in Iberia. Nat. Ecol. Evol. 6, 1644–1657. https://doi.org/10.1038/s41559-022-01861-5.
Vita-Finzi, C., Higgs, E.S., Sturdy, D., Harriss, J., Legge, A.J., Tippett, H., 1970. Prehistoric economy in the mount carmel area of Palestine: site catchment analysis. Proc. Prehist. Soc. 36, 1–37. https://doi.org/10.1017/S0079497X00013074.
Vrac, M., Marbaix, P., Paillard, D., Naveau, P., 2007. Non-linear statistical downscaling of present and LGM precipitation and temperatures over Europe. Clim. Past 3, 669–682. https://doi.org/10.5194/cp-3-669-2007.
Winterhalder, B., 1986. Diet choice, risk, and food sharing in a stochastic environment. J. Anthropol. Archaeol. 5, 369–392. https://doi.org/10.1016/0278-4165(86)90017-6.
Winterhalder, B., Lu, F., Tucker, B., 1999. Risk-senstive adaptive tactics: models and evidence from subsistence studies in biology and anthropology. J. Archaeol. Res. 7, 301–348. https://doi.org/10.1007/BF02446047.
Wolff, E.W., Chappellaz, J., Blunier, T., Rasmussen, S.O., Svensson, A., 2010. Millennial-scale variability during the last glacial: the ice core record. Quat. Sci. Rev., Vegetation Response to Millennial-scale Variability during the Last Glacial 29, 2828–2838. https://doi.org/10.1016/j.quascirev.2009.10.013.
Wickham, H., 2016. ggplot2: Elegant Graphics for Data Analysis. Springer-Verlag, New York. ISBN 978-3-319-24277-4. https://ggplot2.tidyverse.org.
Wisz, M.S., Guisan, A., 2009. Do pseudo-absence selection strategies influence species distribution models and their predictions? An information-theoretic approach based on simulated data. BMC Ecol. 9, 8. https://doi.org/10.1186/1472-6785-9-8.
Yaworsky, P.M., Nielsen, E.S., Nielsen, T.K., 2024. The Neanderthal niche space of Western Eurasia 145 ka to 30 ka ago. Sci. Rep. 14, 7788. https://doi.org/10.1038/s41598-024-57490-4.